

REDDISH-ORANGE EMITTING THERMALLY STABLE Sm^{3+} DOPED $\text{Sr}_2\text{LaSbO}_6$ PHOSPHOR FOR APPLICATIONS IN W-LEDs

A THESIS

**SUBMITTED IN PARTIAL FULFILMENT OF THE REQUIREMENTS FOR
THE AWARD OF THE DEGREE OF
MASTER OF SCIENCE**

**IN
PHYSICS**

SUBMITTED BY:

SHIKHA VERMA (23/MSCPHY/62)

LABHANSH CHAURASIA (23/MSCPHY/29)

Under the supervision of

Prof. A.S. Rao



DEPARTMENT OF APPLIED PHYSICS

DELHI TECHNOLOGICAL UNIVERSITY

(Formerly Delhi College of Engineering) Bawana Road, Delhi-110042

CANDIDATES'S DECLARATION

We hereby certify that the Project Dissertation titled “**Reddish-Orange emitting thermally stable Sm³⁺ doped Sr₂LaSbO₆ phosphor for applications in w-LEDs**” which is submitted by,

SHIKHA VERMA (2K23/MSCPHY/62) and LABHANSH (2K23/MSCPHY/29), Department of Applied Physics, Delhi Technological University, Delhi in partial fulfilment of the requirement for the award of the degree of Master of Science, is a record of the project work carried out by the students under our supervision.

To the best of our knowledge, this work has not been submitted in part or full for any Degree or Diploma to this University or elsewhere.

Place: Delhi

Date: 20 MAY 2025



SHIKHA (23/MSCPHY/62)



LABHNASH (23/MSCPHY/29)

DELHI TECHNOLOGICAL UNIVERSITY

(Formerly Delhi College of Engineering)

Shahbad Daultapur, Main Bawana Road, Delhi-42

CERTIFICATE

Cerified that the SHIKHA VERMA (23/MSCPHY/62) and LABHNASH CHAURASIA (23/MSCPHY/29) have carried out their search work presented in this thesis entitled “**Reddish-Orange emitting thermally stable Sm^{3+} doped $\text{Sr}_2\text{LaSbO}_6$ phosphor for applications in w-LEDs**” for the award of the degree of Master of Science from Department of Applied Physics, Delhi Technological University, Delhi under my supervision. The thesis embodies results of original work, and studies are carried out by the students themselves and the contents of the thesis do not form the basis for the award of any other degree to the candidates or to anybody else from this or any other University/Institution.



Signature

Prof. A.S. Rao,

Department Department of Applied Physics
Delhi Technological University, Delhi, India

DATE: 20/05/2025

ACKNOWLEDGEMENT

We extend our heartfelt gratitude to our supervisor, Prof. A. S. Rao (Department of Applied Physics), for granting us the invaluable opportunity to work in the Materials and Atmospheric Science Research Laboratory. His exceptional guidance, unwavering support, and insightful feedback have been instrumental in the completion of this work. We deeply appreciate his valuable time, thoughtful suggestions, and meticulous review of our manuscripts. His patience and dedication during the writing process have taught us essential nuances that we will carry forward. Prof. Rao's inspiring approach to scientific inquiry made this research journey both enriching and enjoyable.

We are also highly grateful to Ms. Sheetal Kumari for her guidance and unwavering support in this journey. We're grateful to the lab staff for fostering a conducive and healthy working environment, which played a vital role in the success of this project. Additionally, we extend our sincere thanks to the faculty members, M.Sc. (Physics) scholars, and members of the Department of Applied Physics, Delhi Technological University, for their encouragement, suggestions, and valuable support throughout.

Finally, we would like to express our deepest appreciation to our parents for their unwavering belief in us and their constant encouragement, which has been our greatest source of strength and motivation.

LIST OF RESEARCH AND PUBLICATIONS

Title of the paper: “Reddish-Orange emitting thermally stable Sm³⁺ doped Sr₂LaSbO₆ phosphor for applications in w-LEDs”

Author(s): Shikha Verma, Labhansh Chaurasia and Prof. A S Rao

Name of the conference: 3rd International conference on Advanced Functional Materials & Devices for sustainable development (AFMD-2025)

Date and venue: 3rd march 2025

Have you registered for the conference? Yes

Status of the paper: Poster presentation

JOURNAL PUBLICATION:

Title of the paper: “Reddish-Orange emitting thermally stable Sm³⁺ doped Sr₂LaSbO₆ phosphor for applications in w-LEDs”

Author(s): Shikha Verma, Labhansh Chaurasia and Prof. A S Rao

Name of the Journal: Journal of Photochemistry & Photobiology, A: Chemistry

Status of the paper (Accepted/Published/Communicated): Published

Date of paper communicated: 27 January 2025

Date of revised paper communicated: 4 March 2025

Date of paper accepted: 22 March 2025

Paper available online: 10 April 2025

CONTENTS:

Index	Page no
ABSTRACT	6
CHAPTER -1 : INTRODUCTION	
1.1 What are phosphors	7-10
1.2 Host matrix and activator ions	11-12
1.3 Double perovskite oxides	12-14
1.4 White LEDs	14-18
1.5 Photoluminescence	18-20
CHAPTER -2 : INSTRUMENTATIONS	
2.1 X-ray diffraction and Diffractometer	21-26
2.2 Photoluminescence and PL - spectroscopy	26-30
CHAPTER -3 : SYNTHESIS	
3.1 The solid state reaction method	31
3.2 Analysis for characterization	32
CHAPTER -4 : RESULTS AND DISCUSSIONS	33-35
	33-34
4.1 The X-ray diffraction analysis	35-36
4.2 Morphological studies for SEM	37-39
4.3 Diffuse reflectance spectra(DRS)	39-42

4.4 Photoluminescence(PL) spectroscopy analysis	42-44
4.5 Colorimetry analysis	45-48
4.6 PL Decay profile analysis	48-49
4.7 TD-PL spectral analysis	
CHAPTER -5 :CONCLUSIONS AND SCOPE OF WORK	50-51
REFERENCES	52-55
PLAGIARISM REPORT	57-61
PROOF OF CONFERENCE PRESENTATION	62
PROOF OF BEST POSTER PRESENTATION	63
PROOF OF JOURNAL PUBLICATION	64
PUBLICATION PROOF	65

LIST OF FIGURES:

Figure 1.1: The visible part of the EM spectrum and some phosphor materials showing

Figure 1.2 : luminescence in different colour ranges

Figure 1.3: various types of phosphors

Figure 1.4: The Rare-earth elements

Figure 1.5: The emission of photons in a phosphor due to excitation by UV/Visible wavelengths.

Figure 1.6: single and double perovskite.

Figure 1.7: the different approaches for white light production

Figure 1.8: the temperatures depicting the quality of white light produced by different sources

Figure 1.9: The common characteristics of a white LED.

Figure 1.10: Photoluminescence in carbon-dots

Figure 1.11: The Jablonski diagram showing photoluminescence occurring in two ways.

Figure 2.1: The **Bragg's law** depicting the diffraction of X-rays from a crystalline plane

Figure 2.2: The principle working of X-ray diffractometer

Figure 2.3: The X-Ray tube

Figure 2.4: The X-Ray diffractometer machine

Figure 2.5: Analysing a peak in XRD data plot

Figure 2.6: Photoluminescence spectrometer

Figure 2.7: Schematic diagram of scanning electron microscopy and SEM machine

Figure 3.1: Flow chart of the process of synthesis of **Sm³⁺ ions activated Sr₂LaSbO₆**

Figure 4.1: The XRD plots of synthesised phosphor and the Reitveld refinement of undoped phosphor

Figure 4.2: SEM analysis

Figure 4.3: EDX image of the doped phosphor

Figure 4.4 : The DRS spectra of Sr₂LaSbO₆

Figure 4.5: The Tauc plots of Sr₂LaSbO₆:xSm³⁺ (x=1.0, 3.0, 4.0, 5.0 mol%)

Figure 4.6: The Excitation spectra and the emission spectra of the synthesised phosphor

LIST OF FIGURES (continued)

Figure 4.7: PL plot analysis

Figure 4.8: CIE chromaticity coordinates of Sm^{3+} ions in $\text{Sr}_2\text{LaSbO}_6$ phosphors

Figure 4.9: The PL decay plots for Sm^{3+} doped $\text{Sr}_2\text{LaSbO}_6$ phosphor

Figure 4.10: The Dependence of lifetime of excited states on the concentration of Sm^{3+} ions according to the Auzel's model

Figure 4.11: The TD-PL intensity variation and analysis.

LIST OF TABLES:

Table-1: The CIE coordinates and CCT values for Sm^{3+} ions doped $\text{Sr}_2\text{LaSbO}_6$ phosphor

Table-2: The excited state lifetime, Non-Radiative rate and luminous efficiency of the SLS:xSm^{3+} phosphor for $x = 1.0, 2.0, 3.0, 4.0$ & 5.0 mol. %

ABSTRACT

A series of Sm^{3+} ions activated $\text{Sr}_2\text{LaSbO}_6$ (SLS) phosphors was synthesised using the traditional solid-state reaction (SSR) method. This work presents $\text{Sr}_2\text{LaSbO}_6$ as a novel host material, in contrast to previously examined Sm^{3+} -doped phosphors. It uses its double perovskite structure and LaO_6 octahedral coordination to improve light efficiency and stability, an aspect not fully investigated in perovskite-based phosphors. The phase purity of the synthesized materials was inspected using X-ray diffraction (XRD) characterization technique. The luminescent properties were analysed by photoluminescence emission and excitation (PL) spectra, temperature dependent PL (TD-PL) and decay curves. The XRD results matched the standard JCPDS suggesting that the prepared samples comprise a pure cubic phase structure. When subjected to 407 nm excitation, the phosphors convey the intensity peaks at 612 nm corresponding to the transition ${}^6\text{G}_{5/2} \rightarrow {}^5\text{H}_{7/2}$. The PL intensity of the sample rises with the increasing concentration of Sm^{3+} ions until concentration quenching resulted at $x = 3.0$ mol%. The stability and activation energy of the phosphor was calculated with the help of temperature dependant photoluminescence and the phosphor was found out to be highly stable at high temperatures. Most white LEDs use a blue LED chip coated with a yellow phosphor (typically YAG:Ce – Yttrium Aluminium Garnet doped with Cerium). This YAG:Ce phosphor converts some of the blue light into longer wavelengths, producing a broad-spectrum white light. However, this method tends to be weaker in the deep red part of the spectrum, making the light appear cooler and sometimes slightly bluish resulting in high CCT and low CRI. In order to address the prevalent problem of weak red component in white LEDs, which frequently results in low colour rendering index (CRI), this study proposes a Sm^{3+} -doped $\text{Sr}_2\text{LaSbO}_6$ phosphor with high reddish-orange emission. With its efficient 406 nm excitation, the phosphor complements commercial near-UV/blue LEDs and is hence ideal for real-world LED applications. With an activation energy of $\Delta E = 0.424$ eV, it has a strong luminous thermal stability that outperforms several previously reported phosphors, guaranteeing better performance in high-temperature lighting and display technologies. Furthermore, the material has excellent colour purity (96%), putting its emission in the warm red-orange region, which is essential for producing high-quality white light in plasma display panels (PDPs) and solid-state lighting (SSL). These properties make this phosphor a highly efficient red-emitting component, significantly improving the color rendering and performance of w-LEDs.

CHAPTER -1 INTRODUCTION

1.1 Phosphors (what are they and why do we need them?)

Light plays a crucial role in our daily lives and has become a significant focus of research in the modern era. Innovations in illumination technology have transformed various fields of science and technology. Over time, the demand for improved lighting systems has driven the development of incandescent and fluorescent lights. The invention of the incandescent lamp by Thomas Edison in 1879 marked a groundbreaking achievement in human progress. However, these early light sources had numerous limitations, such as voltage distortion, shorter life span, high cost and low efficiency. Since a light resource is not needed to just be efficient but also low at cost of manufacturing, hence the correction of such drawbacks further led to the discovery of phosphor materials which are still a great source of innovation for human society in terms of energy resources and technology even after a century of invention [1].

Phosphors are the materials capable of showing luminescence upon excitation from an external source. They are capable of emitting not just any light but the light in the wavelength in the **visible range** of electromagnetic spectrum which is 380 to 750 nanometres. This range (300 nm-750nm) of the Electromagnetic spectrum (figure 1.1) is the only part which can be sensed by the human eyes and hence are perceived in the form of various colors. Conclusively, we require some material which can execute the emission of the visible light in an efficient, cost effective, environment friendly and highly radiant.

Luminescence is a phenomenon of emission of the light from a substance not due to the presence of high temperatures but other phenomena like atomic transitions, pressure, electrical and chemical responses[2]. The term *luminescence* was first introduced by Eilhard Weidemann in 1888. Derived from the Latin word *lumin*, meaning light, the term describes the emission of radiation by certain materials known as phosphors. This phenomenon represents a unique interaction between matter and energy. These materials, also referred to as luminophores, possess the remarkable ability to convert energy from absorbed photons into visible light. The phenomenon of luminescence can be categorized in two forms : (i) **Fluorescence** and (ii) **Phosphorescence**. In fluorescence, luminescence occurs almost instantaneously after the

absorption of incident radiation and ceases just as quickly. Typically, the emitted radiation has a longer wavelength than the incident radiation. In contrast, phosphorescence is characterized by a delayed emission following the absorption of radiation. This delay can vary significantly, lasting from several minutes to a few hours, depending on the specific host material and activator used.

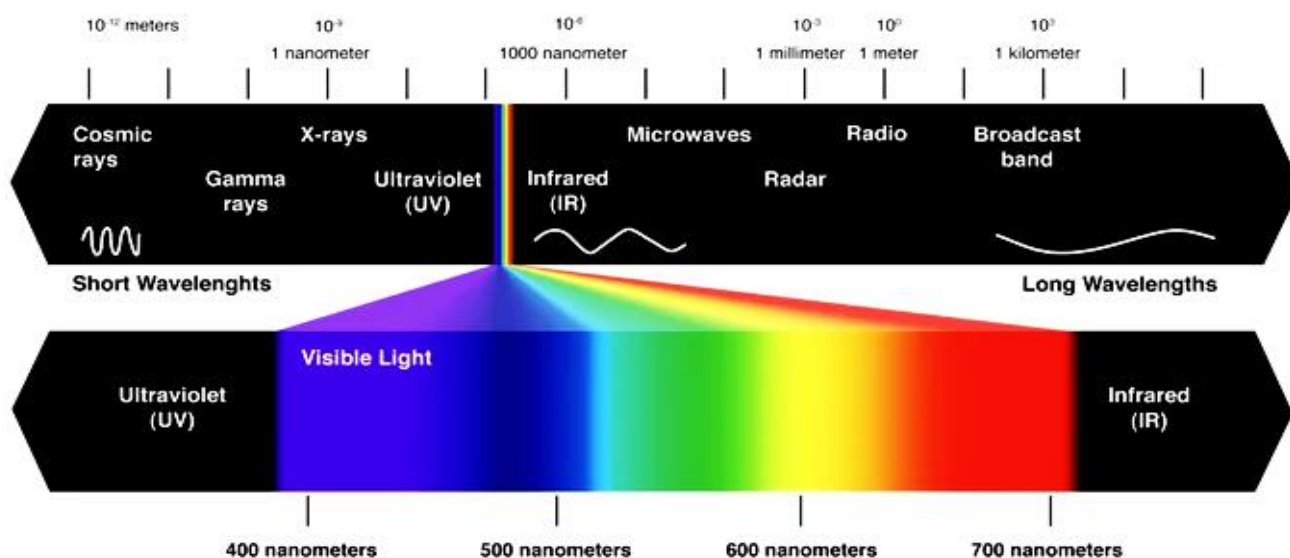


Figure 1.1: The visible part of the EM spectrum and some phosphor materials showing



luminescence

Figure 1.2 : luminescence in different colour ranges On the basis of chemical composition, phosphors can be categorized into **organic and inorganic phosphors**.

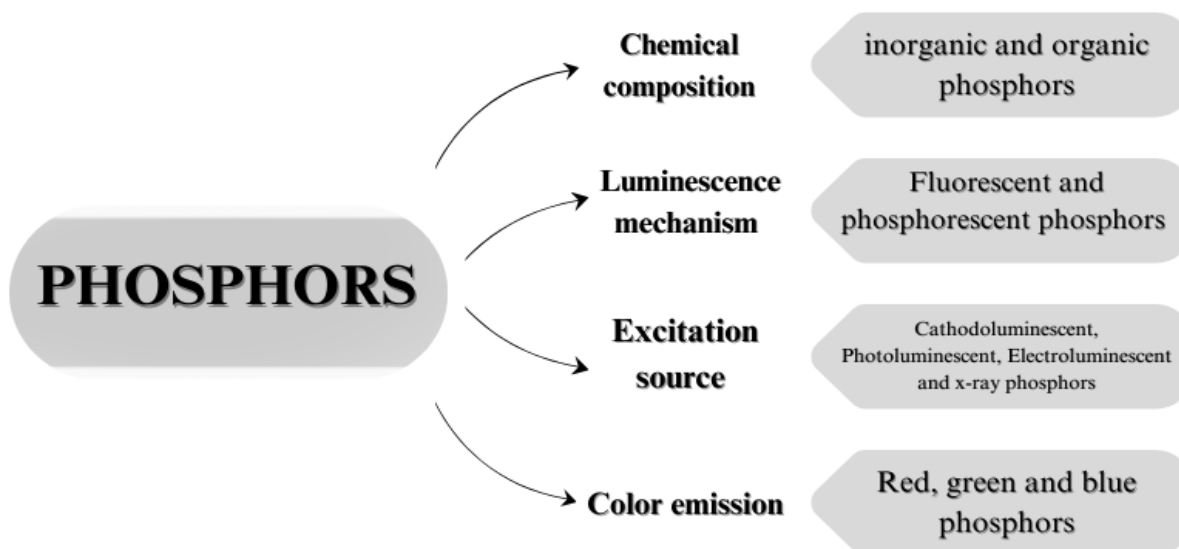


Figure 1.3: various types of phosphors

As shown in figure 1.3. We have made use of the **inorganic phosphors** in this paper. There are multiple methods of synthesis for phosphors. The very basic principle underlying the synthesis of the phosphor is the incorporation of the **Activator ions** into a **Host matrix**. The process of synthesis requires extensive efforts. In order to perform research on phosphors, one needs to have a functional laboratory with high purity maintenance in the lab rooms for synthesising high purity phosphors. The lab should contain furnaces capable of reaching high temperatures such as 1700C for heat treatments like calcination and sintering. [3,4]

Phosphor formulations often comprise more than four elements, making it challenging to produce uniform, single-phase powders. The luminescence efficiency of these materials is governed by their properties, which are influenced by factors such as atomic structure, composition, microstructure, defects, and interfaces—all of which are determined by the synthesis process.

There are various types of host materials used for phosphors including **oxides**, aluminates, silicates, sulfides, tungstates, alumino-silicates, and nitrides, among others. In addition to these hosts, a small amount of activator ions is typically incorporated to enhance their luminescent properties.

The activator ions used are the **Rare-earth** element ions which are also known as the transition metal ions. These activator ions are primarily responsible for the illumination of phosphors at various color ranges. [5]

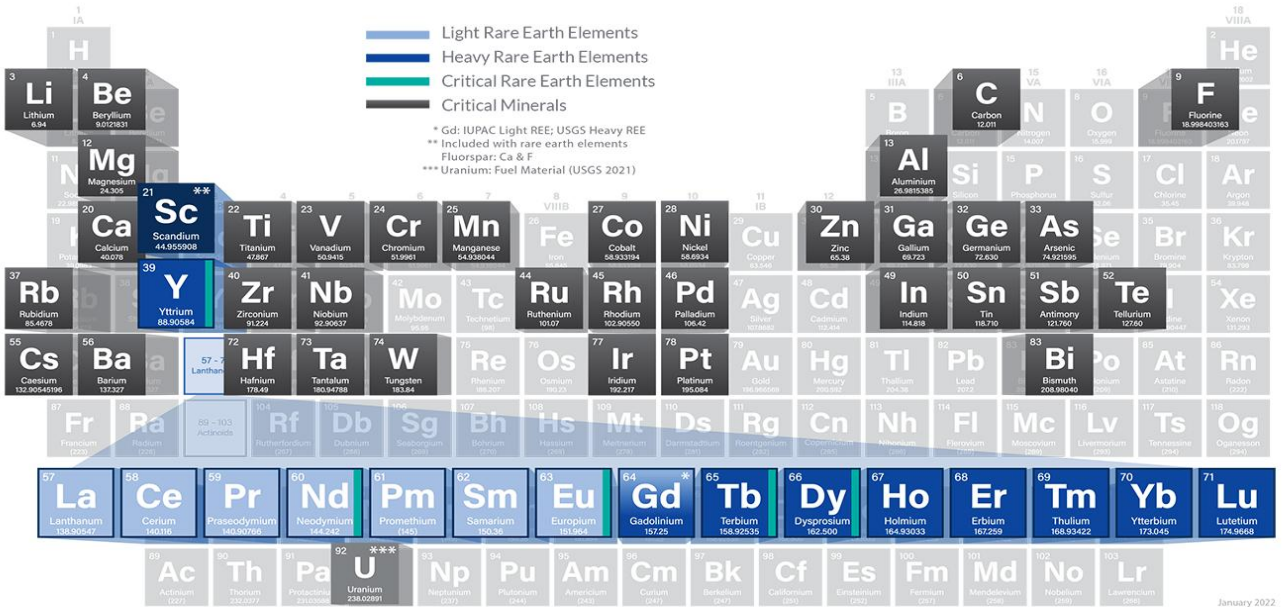


Figure 1.4: the elements in blue highlight show the Rare-earth elements

1.2 Host matrix and activator ions for the phosphors

The Rare-earth activated phosphors have different kinds of properties. A host material is chosen and designed in such a way that it incorporates divalent and trivalent rare-earth ions into their lattices, which are often referred to as impurities or activator ions. When exposed to UV or visible light—or another excitation source, depending on the type of phosphor—activator ions absorb the energy, transition to an excited state, and then relax to a lower energy state, emitting a photon in the process. The emitted photons usually lie in the visible wavelengths depending on the properties of the activated ions[2]. The **efficiency** of the phosphor is defined as the amount of energy emitted compared to the energy used to excite the material. Since some energy is lost due to Non-radiative transitions as well, hence the efficiency of phosphors are not 100%.

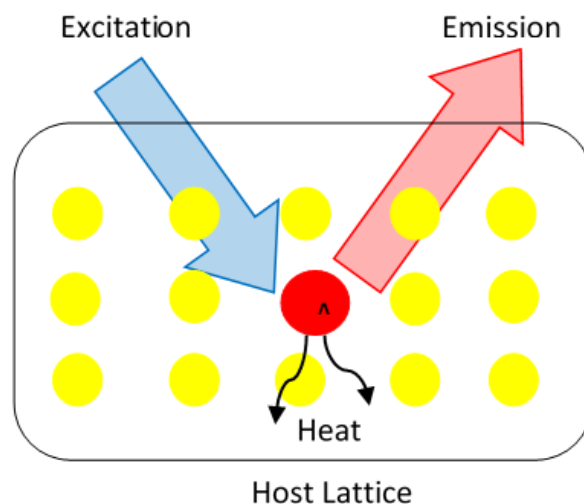


Figure 1.5: The emission of photons in a phosphor due to excitation by UV/Visible wavelengths.

Other than phosphor efficiency, the properties to look for in an **ideal phosphor** are its

- High Thermal Stability,
- Color Quality,
- Color Rendering Index (Cri),
- Color Correlated Temperature(Cct)
- Environment Friendliness And Cost Effectiveness
- and other optical properties such as emission wavelength, quenching concentrations, and luminescent lifetime, etc.

The activator functions as a dopant, introduced into the crystal structure of the host material to induce the desired type of inhomogeneity. Activators play a pivotal role in influencing emission delay time and are crucial in determining the concentration within the crystal lattice. While the host material is generally microcrystalline and transparent to visible light, the activators are responsible for both absorbing and emitting radiation.

By collecting and amplifying stimulating radiation, activators facilitate the transition to an excited state. However, not all ions or elements exhibit luminescence, as this property depends on specific factors that govern the ability of luminescent compounds to convert light. Recently, there has been growing interest in the luminescence of trivalent rare-earth ions (e.g., Sm^{3+} , Dy^{3+} , and Eu^{3+}) in silicates. These ions offer excellent chemical and thermal stability, broad UV

transparency, high luminous efficiency, and low composite temperatures, making them highly suitable for advanced lighting and display applications.

1.3 Double perovskite oxides:

Double perovskite oxides are an advanced class of materials having **general formula** $A_2BB'O_6$ where the sites A are occupied by the alkaline earth metals (Sr, Ba, Ca etc) or the lanthanides and B and B' sites are primarily occupied by transition metals (Sb, La, Mn, Sc, Ni etc). The double perovskite compounds (DPCs) are composed of the two single perovskite structures (SPSs) having formula ABO_3 . As shown in figure 1.6, the formation of DCPs is a simple alternative arrangement of the single perovskite structures. The alternation of B and B' cations in the lattice creates a **rock-salt-type** arrangement within the perovskite framework. This ordering has significant influence on the electronic, magnetic, and optical properties of the material making it a good candidate for the host matrix of the phosphors. Depending on the size, charge, and compatibility of the cations, the symmetry of the double perovskite lattice can range from **cubic to monoclinic**. [6–8]

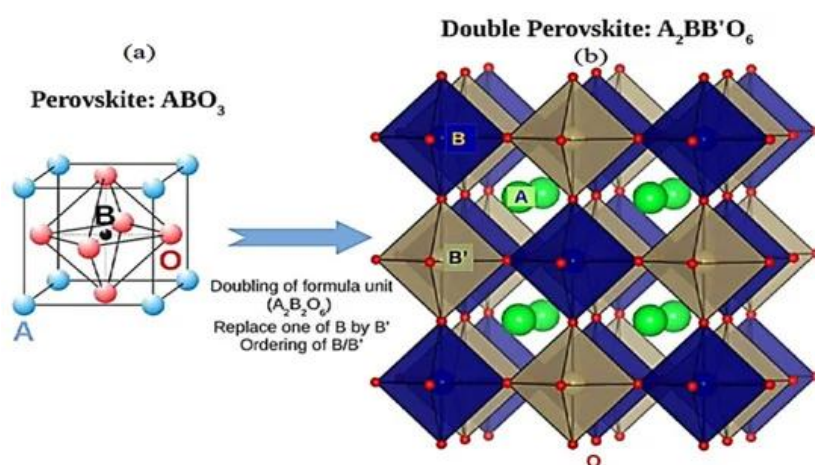


Figure 1.6: (a) A single perovskite structure (SPS) and (b) A double perovskite structure (DPC) made out of two SPS

Numerous double perovskites can be synthesised using the solid-state reaction method. Their crystal structure, phase formation and the purity can be analysed using x-ray diffractometers (XRD) and scanning electron microscopy (SEM) for particle size and surface morphology.

Properties of double perovskite oxides:

1. Electronic Properties:

- They can exhibit metallic, semiconducting, or insulating behavior, depending on the cation composition.
- Many double perovskites show high charge mobility and are being explored for electronic and energy applications.

2. Magnetic Properties:

- Display diverse magnetic behaviors, including ferromagnetism, antiferromagnetism, and ferrimagnetism.
- Some are half-metallic, making them attractive for spintronic devices.

3. Optical Properties:

- Known for their luminescence and photoresponse, they are used in light-emitting diodes (LEDs) and photocatalysis.
- Certain double perovskites have excellent bandgap tunability for applications in photovoltaics.

4. Thermal and Catalytic Properties:

- Exhibit high thermal stability and catalytic activity, making them suitable for fuel cells, CO₂ reduction, and water splitting.

Applications:

1. **Renewable Energy:** Used in photovoltaic cells, thermoelectrics, and fuel cells due to their tunable bandgaps and high stability.
2. **Spintronics:** Half-metallic and magnetic double perovskites are promising for spin-based memory and logic devices.
3. **Catalysis:** Their activity in oxygen evolution/reduction and CO₂ reduction makes them valuable for environmental applications.
4. **Optoelectronics:** Double perovskites with tailored bandgaps are used in LEDs, lasers, and other light-emitting devices.

1.4 White LEDs (WLEDs) :

The Need and Synthesis of White LEDs in Material Sciences:

White light-emitting diodes (LEDs) have revolutionized lighting technology, offering **energy efficiency**, **durability**, and **eco-friendliness** compared to traditional incandescent and fluorescent lighting. The growing demand for sustainable and high-performance lighting solutions has driven extensive research into the development of white LEDs in material science. The need for white LEDs stems from their superior energy efficiency, consuming up to 80% less power while offering comparable or better luminosity. Their long lifespan reduces maintenance costs and waste, making them an environmentally responsible choice. Furthermore, white LEDs exhibit high luminous efficacy, rapid response times, and excellent reliability, making them indispensable for applications in residential, industrial, and automotive lighting, as well as in display technologies[9–11] .

The synthesis of white LEDs involves two primary approaches: **phosphor-based** and **phosphor-free** methods.

In phosphor-based white LEDs: a blue or ultraviolet LED excites a phosphor material, typically rare-earth-doped compounds such as YAG:Ce (yttrium aluminum garnet doped with cerium), to produce white light. This approach is widely used due to its simplicity and efficiency, although it may face limitations in achieving high color rendering index (CRI) and thermal

stability. Researchers are actively exploring alternative phosphor compositions, such as silicates, nitrides, and oxynitrides, to overcome these challenges[9–12].

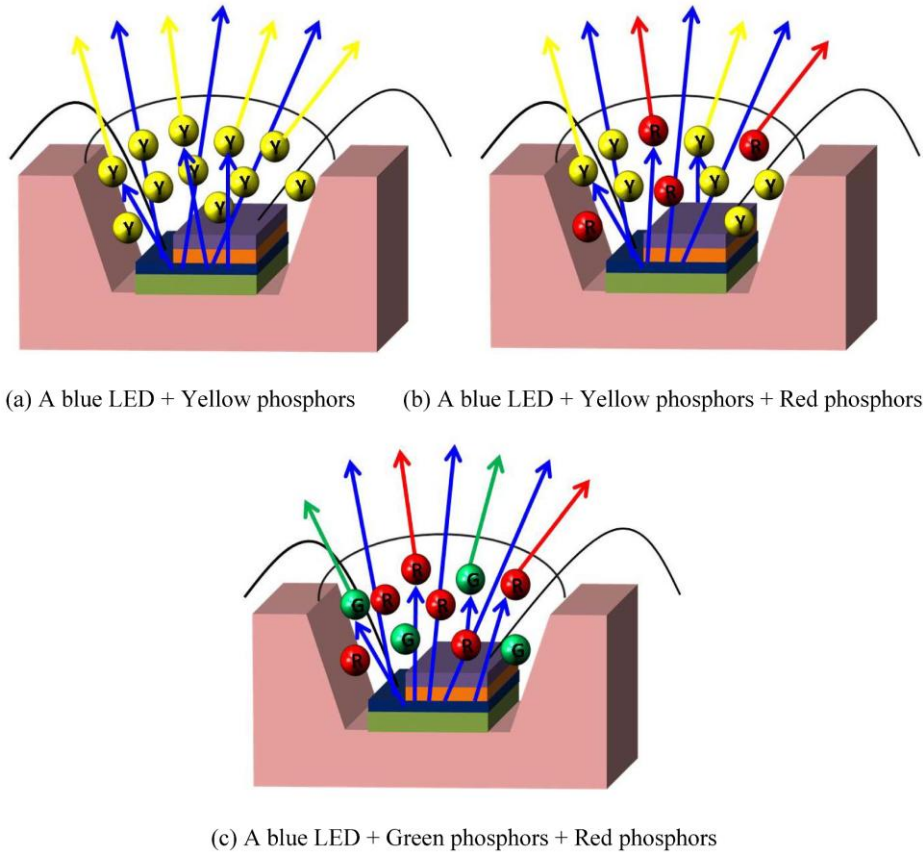


Figure 1.7: the different approaches for white light production

Phosphor-free methods, on the other hand, generate white light by combining red, green, and blue (RGB) LEDs. This approach enables precise control over the emitted spectrum, resulting in superior color rendering and tunability. However, balancing the intensity and stability of individual LEDs remains a challenge, requiring innovations in material engineering.

Some **parameters** are crucial to analyse in the white LEDs synthesised such as:

CRI (Color Rendering Index):

Definition: CRI is a measure of how accurately a light source reveals the colors of objects compared to a natural light source (such as sunlight). It is expressed as a value on a scale of 0 to 100[13].

Importance: A high CRI (closer to 100) means colors appear more natural and vibrant under the light source. Lower CRI values result in distorted or unnatural color rendering.

Applications:

- High CRI (90+): Required in applications like photography, art galleries, medical lighting, and retail.
- Moderate CRI (70–89): Suitable for general residential, commercial, or office lighting.

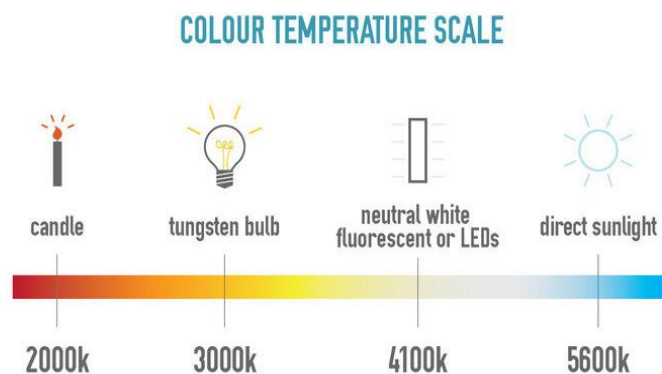


Figure 1.8: the temperatures depicting the quality of white light produced by different sources. The Common CCT values range from 2700 K (warm white) to 6500 K (daylight white)..

CCT (Correlated Color Temperature):

Definition: CCT describes the color appearance of the light emitted by a source, measured in Kelvin (K). It indicates whether the light appears warm (yellowish) or cool (bluish).

CCT Scale: (see figure 1.8)

- **Warm White (2000–3000 K):** Produces a cozy, inviting yellowish light. Commonly used in homes, restaurants, and hotels.
- **Neutral White (3100–4500 K):** Balanced light with a neutral tone, suitable for offices and retail spaces.
- **Cool White (4600–6500 K):** Bright, bluish-white light that mimics daylight. Used in hospitals, industrial areas, and outdoor spaces.

- **Applications:** Choosing the right CCT enhances the ambiance and functionality of a space. For instance, warm white is preferred for relaxation, while cool white improves focus and visibility.

Both **CRI** and **CCT** are critical parameters for assessing and optimizing the quality of light in LED-based applications.

In material science, the development of white LEDs focuses on optimizing the performance of luminescent materials and improving energy efficiency. Key research areas include enhancing thermal stability, minimizing non-radiative energy losses, and increasing quantum efficiency. Additionally, the integration of nanomaterials and advanced fabrication techniques offers promising pathways for achieving higher efficiency and stability in next-generation white LEDs[14–17].



Figure 1.9: The common characteristics of a white LED.

White LEDs represent a remarkable confluence of scientific innovation and environmental responsibility. As material science continues to advance, white LED technology is set to play a pivotal role in creating sustainable, energy-efficient lighting solutions for a brighter and greener future.

1.5 Photoluminescence:

Photoluminescence (PL) is a light emission process that occurs when a material absorbs photons (light energy) and re-emits them. This phenomenon is widely studied in material science for its applications in optoelectronics, sensors, and light-emitting devices.



Figure 1.10: Photoluminescence in carbon-dots

The process begins with the absorption of incident photons, which excite electrons in the material from their ground state to a higher energy state. After a brief period, these excited electrons return to their ground state, releasing energy in the form of light. The wavelength of the emitted light is typically longer than the absorbed light due to energy losses from non-radiative processes[14–21].

Photoluminescence can be categorized into two types: **fluorescence** and **phosphorescence**. In fluorescence, light emission occurs almost immediately (within nanoseconds) after excitation, while in phosphorescence, emission is delayed and can last from milliseconds to hours, depending on the material. See figure 1.11.

In **fluorescence**, when a photon excites an electron in a molecule or material, the electron is elevated from its ground state (S_0) to a higher electronic energy state (S_1 or S_2). The molecule quickly loses vibrational energy and stabilizes in the lowest vibrational level of the excited state (S_1). The electron then transitions back to the ground state, emitting a photon in the process.

Fluorescence is an extremely fast process, with emission occurring within nanoseconds (10^{-9} seconds) of photon absorption.

The emitted light generally has a longer wavelength (lower energy) than the absorbed light due to vibrational energy losses during relaxation. This is known as the **Stokes shift**.

Phosphorescence involves a similar excitation process, where electrons absorb photons and transition to an excited state. However, in this case, the excited electron undergoes intersystem crossing to a triplet state (T_1), which has a different spin multiplicity than the ground state. Transitioning back to the ground state from the triplet state is "forbidden" in quantum mechanical terms, making the process slower.

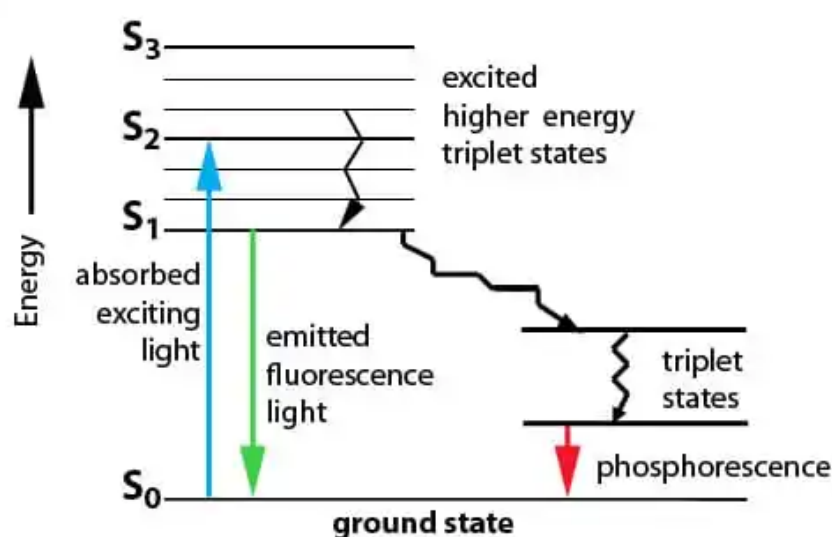


Figure 1.11: The Jablonski diagram showing photoluminescence occurring in two ways

Due to the forbidden nature of the triplet-to-singlet transition, phosphorescence emission is delayed and can last from milliseconds to several hours[4].

Similar to fluorescence, the emitted light has a longer wavelength than the absorbed light. However, due to the triplet state, phosphorescence typically has an even longer wavelength than fluorescence.

PL is a valuable tool for studying the electronic structure, defects, and optical properties of materials. It is commonly used to characterize semiconductors, nanomaterials, and phosphors.

Advances in photoluminescent materials have enabled the development of high-efficiency LEDs, solar cells, and bio-imaging technologies, demonstrating the importance of this phenomenon in both research and practical applications[11,12,16].

CHAPTER -2 : INSTRUMENTATION

2.1 X-Ray Diffraction:

X-ray diffraction (XRD) is a powerful analytical technique used to study the atomic and molecular structure of crystalline materials. It is based on the phenomenon of diffraction, which occurs when X-rays interact with a crystal lattice. The scattered X-rays form a pattern that provides valuable information about the material's structure, phase, and properties.

Principle of working XRD:

XRD works on the principle of **Bragg's Law**, which describes the constructive interference of X-rays reflected from parallel crystal planes. According to Bragg's Law[16]:

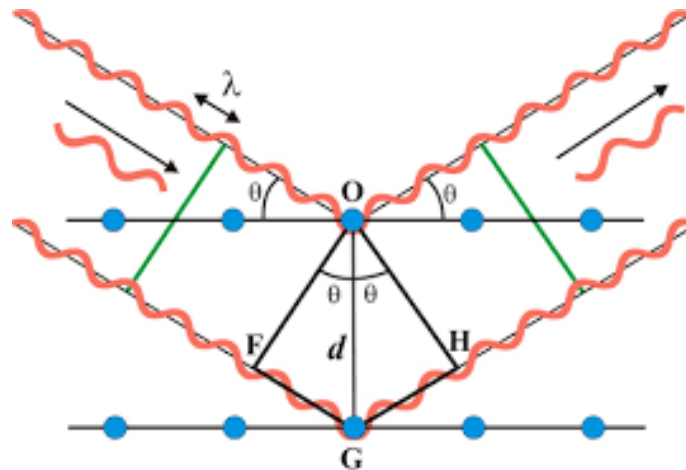


Figure 2.1: The **Bragg's law** depicting the diffraction of X-rays from a crystalline plane

Process of XRD:

1. **X-ray Generation:** X-rays are produced in an X-ray tube, where high-energy electrons bombard a metal target (commonly Cu or Mo).
2. **Sample Interaction:** The collimated X-ray beam is directed onto the crystalline sample. The interaction produces scattered X-rays based on the crystal's lattice structure.
3. **Detection:** A detector records the intensity of diffracted X-rays as a function of the diffraction angle (2θ).

4. **Data Analysis:** The diffraction pattern, which consists of peaks corresponding to specific crystal planes, is analyzed to extract information about the crystal structure, phase composition, and other properties[9,16,22].

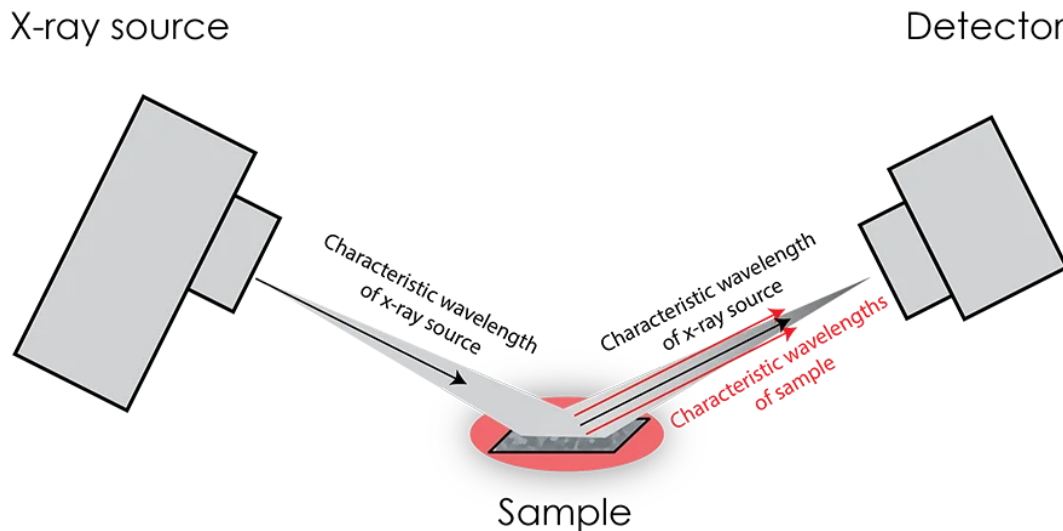


Figure 2.2: The principle working of X-ray diffractometer

Applications of XRD: XRD is extensively used in material science, geology, chemistry, and engineering. It helps identify crystalline phases, determine lattice constants, analyse crystallite size, and detect structural defects. Non-destructive and precise, XRD is invaluable for studying both natural and synthetic materials, from minerals and metals to pharmaceuticals and polymers.

This technique has greatly advanced our understanding of material properties and behavior.

Working of an X-Ray Diffractometer (XRD) Machine: An X-ray diffractometer (XRD) is a powerful analytical tool used to determine the crystalline structure, phase composition, and lattice parameters of materials. Its working principle is based on **Bragg's Law**, which relates the diffraction of X-rays by crystal planes to their spacing.

- **X-Ray Generation:** The process begins with the production of X-rays in an X-ray tube. Electrons, accelerated under high voltage, collide with a target material (commonly copper

or molybdenum), generating X-rays through Bremsstrahlung and characteristic emission processes. These X-rays are collimated and directed at the sample.

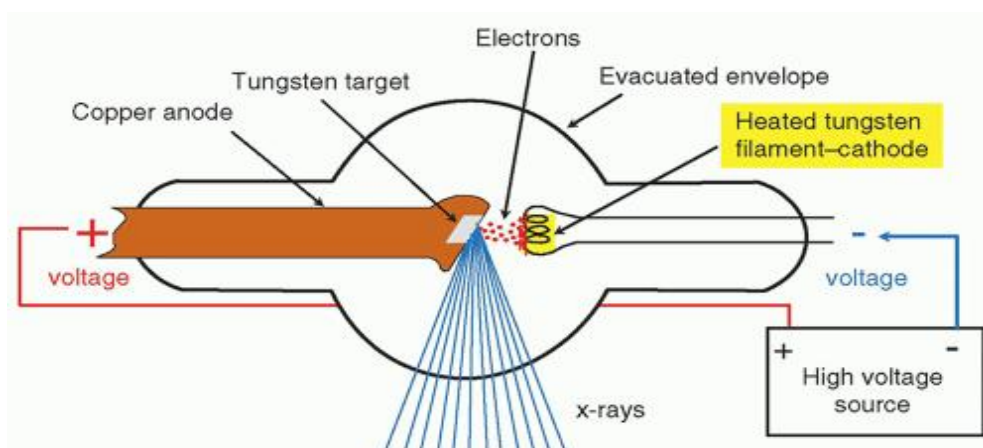


Figure 2.3: The X-Ray tube

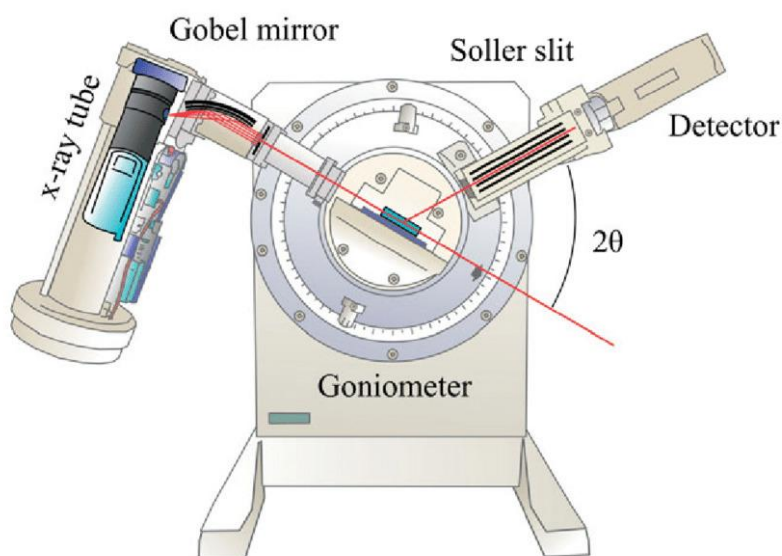


Figure 2.4: The X-Ray diffractometer machine

- **Sample Interaction:**

The sample, typically in powdered or thin-film form, is mounted on a holder. When the collimated X-ray beam strikes the crystalline sample, the crystal planes act as diffraction gratings, scattering the X-rays in specific directions. The scattered X-rays interfere

constructively or destructively, depending on the spacing of the crystal planes and the incident angle. Constructive interference follows **Bragg's Law**: [23,24]

$$n\lambda = 2 d \sin \theta \quad (1)$$

Where n is the order of diffraction, λ is the X-ray wavelength, d is the interplanar spacing, and θ is the diffraction angle.

- **Detector and Data Collection**

A detector, positioned to rotate around the sample, records the intensity of diffracted X-rays at various angles (2θ). The resulting diffraction pattern is a plot of intensity versus angle, with peaks corresponding to specific crystal planes.

- **Data Analysis**

The diffraction pattern is analyzed to identify the material's crystal structure, phase composition, and other properties. Software tools compare the patterns with reference databases to determine the material's identity.

XRD is widely used in materials science, geology, chemistry, and engineering for characterizing crystalline substances and understanding their structural properties. It is a non-destructive, precise, and versatile technique.

X-ray diffraction (XRD) analysis provides a wealth of information about the structural and physical properties of crystalline materials. The key depictions that can be drawn from XRD data include:

1. Phase Identification

- **What It Reveals:** The presence of distinct diffraction peaks corresponds to the crystal planes of specific phases. By comparing the experimental pattern with reference databases (e.g., ICDD), the material's crystalline phases can be identified.
- **Application:** Determining single or multi-phase compositions in alloys, ceramics, minerals, and polymers.

2. Lattice Parameters

- **What It Reveals:** The interplanar spacing (d) calculated using **Bragg's Law** helps determine the unit cell dimensions (lattice constants) of the crystal.
- **Application:** Understanding crystal structure (e.g., cubic, tetragonal, hexagonal) and confirming structural modifications like doping or alloying.

3. Crystallite Size

- **What It Reveals:** The width of the diffraction peaks (via the Scherrer equation shown below) provides an estimate of the average size of crystallites or grains in the material[23–25].

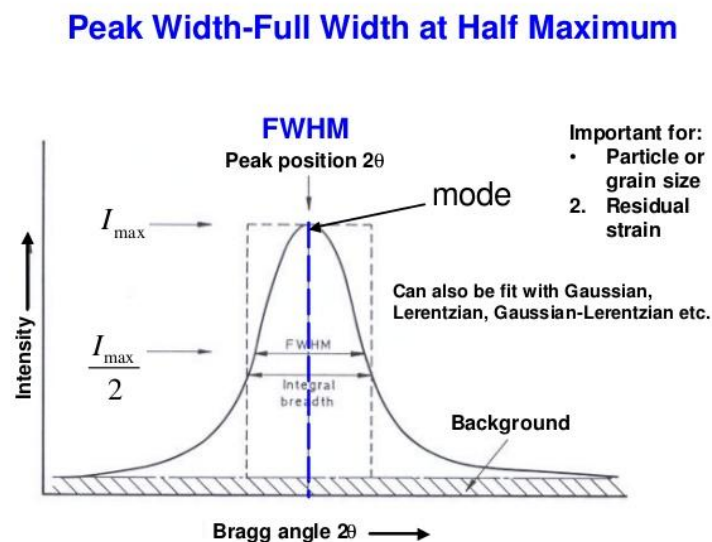


Figure 2.5: Analysing a peak in XRD data plot

$$\text{Crystallite Size} = K\lambda / \beta \cos\theta$$

Where K is the shape factor, λ is the X-ray wavelength, β is the full width at half maximum (FWHM), and θ is the diffraction angle.

- **Application:** Analysis of nanomaterials, thin films, and grain refinement in metals.

4. Strain and Defects:

- **What It Reveals:** The shift, broadening, or asymmetry of diffraction peaks indicates strain, lattice distortion, or crystal defects in the material.
- **Application:** Investigating residual stress in metals, structural integrity, and defect engineering in semiconductors.

5. Preferred Orientation (Texture)

- **What It Reveals:** Anisotropy in peak intensities reflects the preferential alignment of crystallites, referred to as texture.
- **Application:** Understanding grain orientation in polycrystalline materials, such as coatings or rolled metals

6. Phase Quantification

- **What It Reveals:** By analyzing peak intensities, the relative amounts of different phases can be quantified.
- **Application:** Determining phase ratios in mixtures, composites, or alloys.

7. Identification of Amorphous Content

- **What It Reveals:** A broad hump in the diffraction pattern indicates the presence of amorphous material alongside crystalline phases.
- **Application:** Studying glasses, polymers, or partially crystalline materials.

8. Symmetry and Space Groups

- **What It Reveals:** Analysis of peak positions and intensities helps determine the symmetry and space group of the crystal structure.
- **Application:** Classifying crystal structures and understanding their physical properties.

2.2 Photoluminescence (PL) Spectroscopy:

Photoluminescence (PL) spectroscopy is an optical technique used to study the electronic and optical properties of materials. It involves the emission of light by a material after it absorbs

photons, making it a non-destructive method for characterizing semiconductors, nanomaterials, and photonic devices.

When a material absorbs light (typically in the ultraviolet, visible, or near-infrared range), electrons in the material are excited from their ground state to higher electronic energy states. After a brief relaxation period, these excited electrons return to their ground state, emitting photons in the process. The emitted light is analyzed to gain insights into the material's properties.



Figure 2.6: Photoluminescence(PL) spectrometer

Key steps in the process:

1. **Excitation:** A light source (e.g., laser or lamp) excites electrons in the material.
2. **Relaxation:** Electrons lose energy via radiative (light-emitting) or non-radiative pathways.
3. **Emission:** Radiative transitions release photons, which are detected and analyzed.

Information Obtained from PL Spectroscopy:

1. **Electronic Structure:** PL spectra reveal bandgap energy, defect states, and excitonic transitions in semiconductors.
2. **Material Quality:** Sharp and well-defined peaks indicate high crystal quality, while broad or shifted peaks suggest defects or impurities.
3. **Defect Analysis:** Non-radiative processes and emissions from defect states can be identified.
4. **Quantum Efficiency:** The intensity of emitted light is used to evaluate the efficiency of photon absorption and emission.
5. **Charge Carrier Dynamics:** The time-resolved PL (TRPL) technique provides insights into carrier lifetimes and recombination mechanisms.

PL spectroscopy is a versatile and indispensable tool in materials science for advancing the development of next-generation photonic and optoelectronic technologies. See figure 2.6, shows a UV-PL spectrometer.

2.3 Scanning electron microscopy (SEM) technique: Scanning Electron Microscopy (SEM) is a powerful imaging technique used to observe the surface morphology and microstructure of materials at very high magnifications. Unlike optical microscopes, SEM uses a focused beam of high-energy electrons to scan the sample surface. When these electrons interact with atoms in the sample, they generate various signals, such as secondary electrons, backscattered electrons, and X-rays, which are collected to produce detailed images and elemental information.

The most commonly detected signals are secondary electrons, which provide high-resolution, three-dimensional-like images of the surface topography. Backscattered electrons, on the other hand, help in distinguishing different phases based on atomic number contrast. Energy-dispersive X-ray spectroscopy (EDS), often attached to SEM systems, allows for elemental analysis of specific areas.

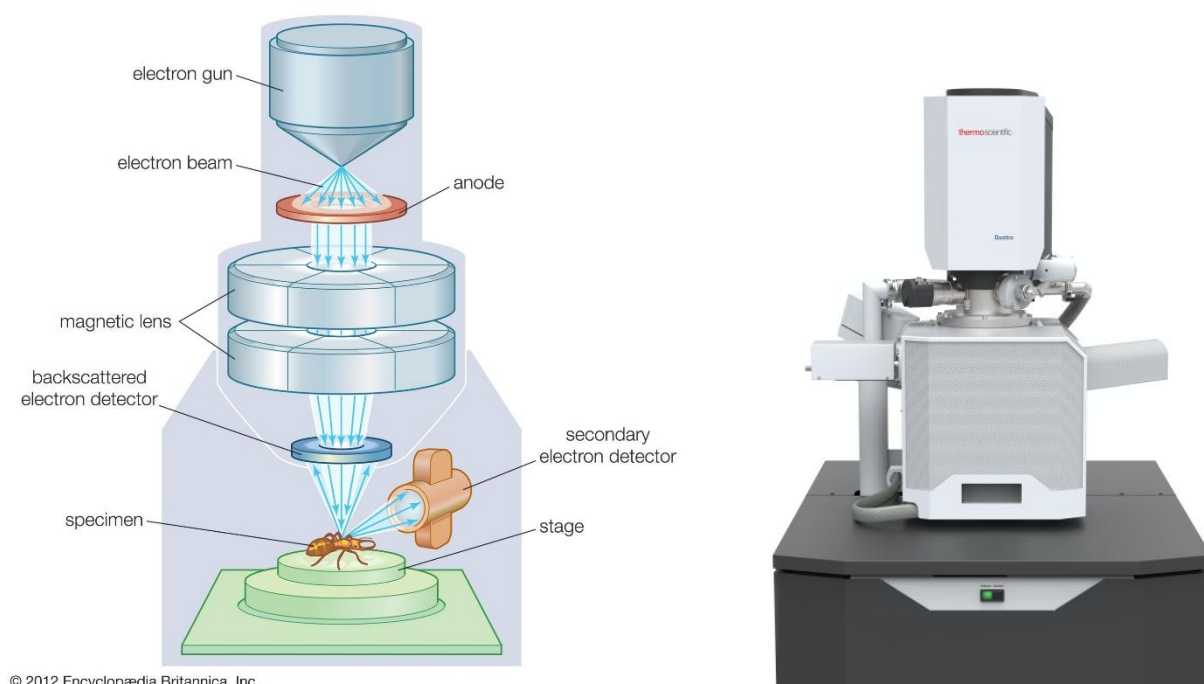


Figure 2.7: Schematic diagram of scanning electron microscopy and SEM machine

How Scanning Electron Microscopy (SEM) Works:

1. **Electron Beam Generation:** SEM begins with the generation of a focused beam of high-energy electrons using an electron gun, typically made of tungsten or a field emission source. These electrons are accelerated and narrowed into a fine beam using electromagnetic lenses.
2. **Scanning the Sample:** The focused electron beam is scanned across the surface of the sample in a raster (grid-like) pattern. This interaction occurs in a vacuum chamber to prevent electron scattering by air molecules.
3. **Electron-Sample Interaction:** When the beam strikes the sample, it interacts with the atoms on the surface, producing various types of signals:
 - **Secondary electrons (SE):** Ejected from the outer shells of atoms, providing detailed surface topography.
 - **Backscattered electrons (BSE):** Reflected from the nucleus, offering compositional contrast (heavier elements appear brighter).

- **Characteristic X-rays:** Emitted when inner-shell electrons are replaced, used for elemental analysis (EDS/EDX).
4. **Detection and Imaging:** Detectors capture these signals and convert them into electrical signals, which are processed to form an image on a computer screen. The brightness and contrast of the image depend on the type and intensity of the detected signal.

SEM requires the sample to be electrically conductive. Non-conductive materials are typically coated with a thin layer of gold, platinum, or carbon. The resolution of SEM can reach down to a few nanometers, making it essential in fields like materials science, nanotechnology, biology, and semiconductor research[8,26–29].

Overall, SEM is a versatile and indispensable tool for analyzing surface structures, detecting defects, and understanding the composition of materials at micro to nanoscale levels.

CHAPTER -3 PROCESS OF SYNTHESIS

3.1 THE SOLID-STATE REACTION METHOD

The solid-state reaction method is a widely used technique for the synthesis of a wide class of materials. It is a widely used technique in materials science for synthesizing crystalline solids, particularly ceramics, oxides, and other inorganic compounds. This method involves the reaction of solid reactants at elevated temperatures to form the desired product[9,30,31].

Here we have synthesised the **Sm³⁺ ions activated Sr₂LaSbO₆ (SLS)** i.e **Sr₂LaSbO₆: xSm³⁺** [**x= 1.0, 2.0, 3.0, 4.0 and 5.0 mol%**] via solid-state reaction (SSR) route. The approach has been shown in figure -3.1.

- i. Selection of Precursors:** The precursors are SrCO₃(99.99%), La₂O₃(99.99%), Sb₂O₅ (99.99%) and Sm₂O₃(99.99%).
- ii. Mixing and grinding:** The precursors are taken in their raw state. The stoichiometric amount of precursors is weighed and further grinded in an Agate mortar and pestle for 1 hour.
- iii. Calcination :** The mixture is then heated at the temperature of 800°C in the furnace for 10 hours.
- iv. Reaction mechanism:** The reaction among the precursors occurs while heating, hence resulting in the formation of the final compound.

- v. **Regrinding and sintering:** the mixture was removed from the furnace and was allowed to cool down at room temperature. The mixture was further regrinded and sintered again for 15 hours at 1300°C.

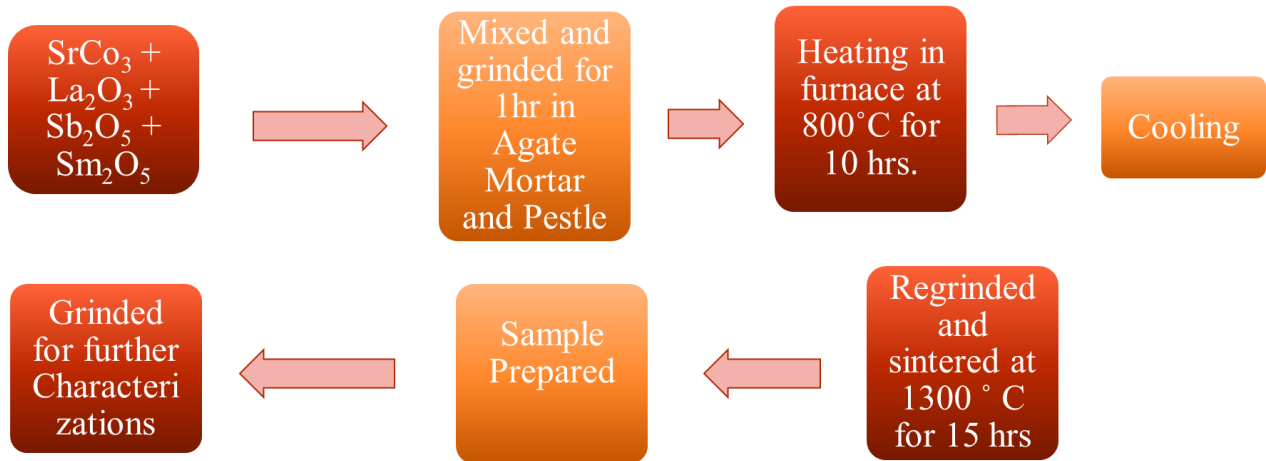


Figure 3.1: Flow chart of the process of synthesis of **Sm³⁺ ions activated Sr₂LaSbO₆**

3.2 Analysis for characterization: The crystal structures of the as-synthesised Sr₂LaSbO₆: xSm³⁺ (1.0 ≤ x ≤ 5.0 mol %, Δx = 1.0 mol %) phosphors were characterized by powder XRD analysis. The X-ray Diffraction pattern has been collected using X-ray (Bruker, model- D8 Advance) Diffractometer (Cu-Kα radiation source, λ = 1.5406 Å) and the data were obtained over the 2θ range of 20°-80°. The PL emission and excitation spectra were captured using a JASCO (FP-8300) Spectrofluorophotometer (1.0 nm resolution)

CHAPTER- 4: RESULTS AND DISCUSSION

4.1 X-RAY DIFFRACTION ANALYSIS:

The figure-4.1 (a) below depicts the XRD data of the synthesised and JCPDS-04-016-9398. The results have shown that the peaks of the synthesised material match with the standard peaks in JCPDS-04-016-9398 plot. The lattice parameters of synthesised phosphor are $a = 0.58613 \text{ nm}$, $b = 0.59220 \text{ nm}$ and $c = 0.83245 \text{ nm}$ with volume $V = 28.89 \text{ nm}^3$. The phosphor has the space group is $P21/n(14)$ and monoclinic structure. the crystallite size has been calculated considering the major peaks of the XRD pattern using Debye-Scherrer formula as shown below[25]:

$$D = \frac{k\lambda}{\beta \cos\theta} \quad (2)$$

Where λ denotes the wavelength of X-ray used (1.54 nm), θ is the angle of diffraction, β represents the full width at half maxima (FWHM), k stands for constant (0.98), D shows the crystallite size. The crystallite size of the undoped $\text{Sr}_2\text{LaSbO}_6$ phosphor was determined to be 31 nm. Figure 19(b) presents the Rietveld refinement of the undoped sample. The goodness-of-fit value (χ^2) obtained is 1.67, which is less than 2, indicating the successful formation of a pure phase in the synthesized material[16,25,32].

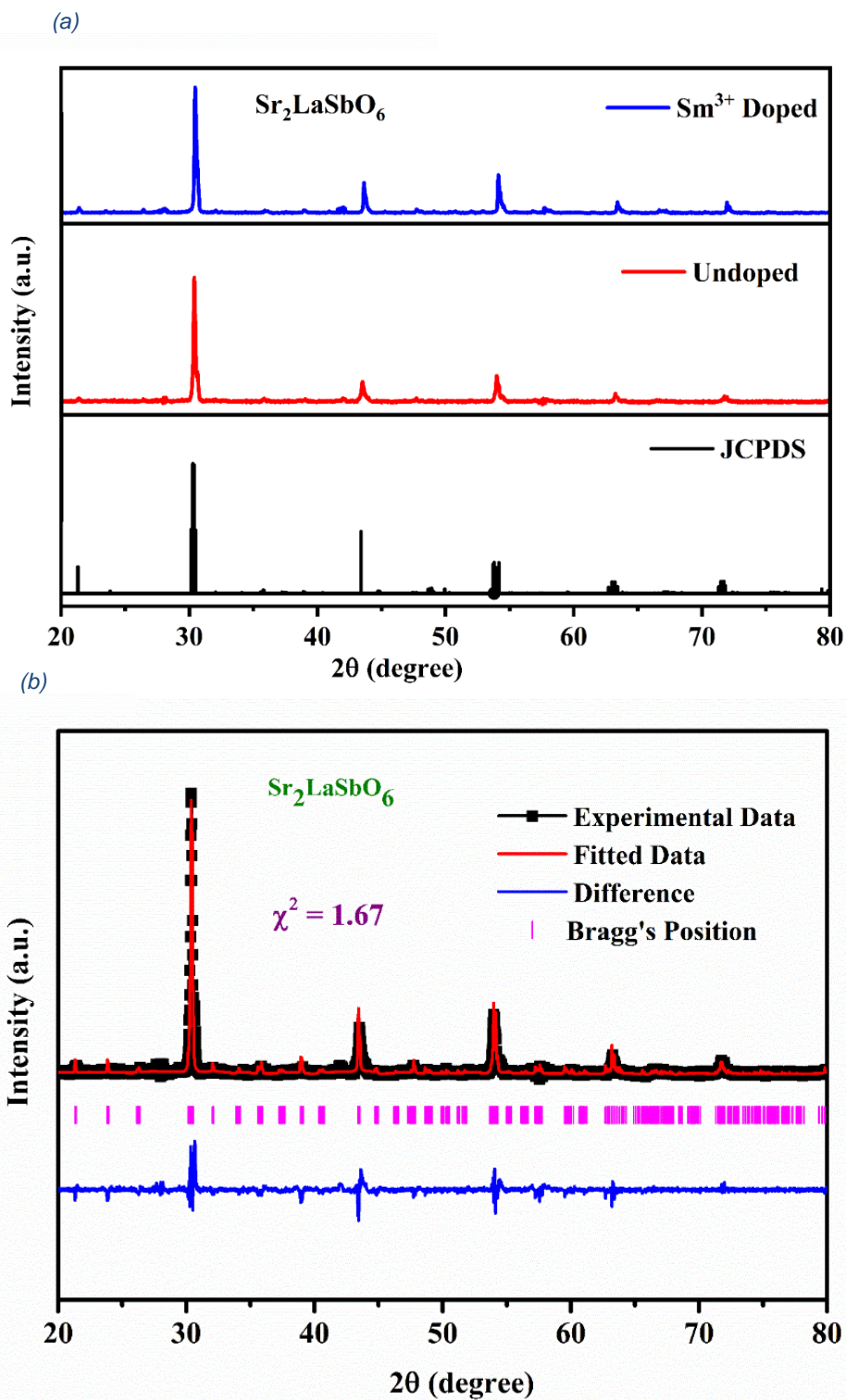


Figure 4.1: (a) The XRD plots of synthesised phosphor undoped and doped with Sm^{3+} ions compared to the standard JCPDS file and (b) the Reitveld refinement of undoped phosphor.

4.2 MORPHOLOGICAL STUDIES FOR SCANNING ELECTRON MICROSCOPY (SEM):

SEM is one of the crucial aspects to consider while studying the properties of a material. In order to investigate the morphology and the particle size of the phosphor, we perform SEM analysis on the as-prepared phosphor. To analyse the morphology of a material using the Scanning Electron Microscopy (SEM) technique, the sample is first carefully prepared, usually by ensuring it is clean and, if it's non-conductive, coating it with a thin conductive layer like gold or carbon. This is important because SEM relies on the interaction of an electron beam with the surface of the material, and a conductive surface helps prevent charging, which can distort the image.

Once the sample is ready, it is placed inside the vacuum chamber of the SEM instrument. A focused beam of electrons is then directed onto the surface. As this beam scans over the sample, it interacts with the atoms at and near the surface, producing various signals, particularly secondary electrons, which are most useful for imaging surface features.

The SEM detects these secondary electrons and uses them to create highly detailed images that reveal the surface morphology—essentially the texture, shape, and arrangement of particles or grains on the material. Through these images, researchers can observe features like grain size, porosity, cracks, surface roughness, and overall structure. This information helps in understanding how the material might perform in various applications, especially where surface characteristics are critical, such as in catalysis, coatings, or electronic devices.

FE-SEM results for the undoped $\text{Sr}_2\text{LaSbO}_6$ and doped $\text{Sr}_2\text{LaSbO}_6$ with 3.0 mol% concentration of Sm^{3+} . As depicted in the figure-4.2(a), the powder phosphors of $\text{Sr}_2\text{LaSbO}_6$ have irregular polyhedral shape with varying particle sizes. The particle sizes lie in the range of 3–6 μm in size, while most commercially available phosphor particles have size in the range of 2–10 μm [22,33,34]. These microscale particles are well-suited for applications such as coatings in display technologies and white LEDs.

Figure-4.3 displays the EDX images of the doped samples, confirming the presence of all the intended precursor elements within the lattice structure.

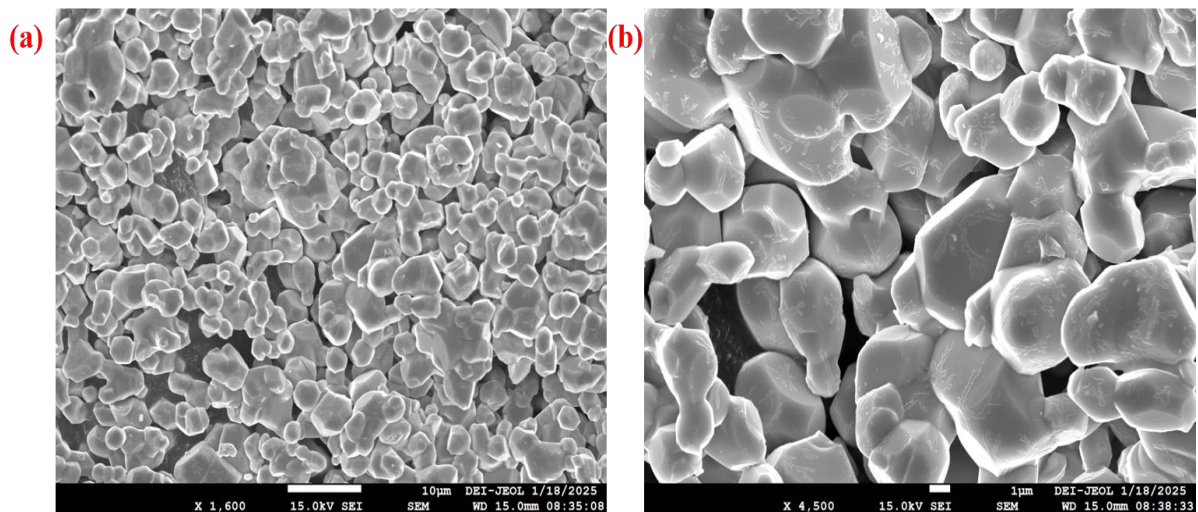


Figure 4.2: SEM images recorded for (a) an un-doped (b) 3.0 mol% of Sm^{3+} ions doped $\text{Sr}_2\text{LaSbO}_6$ phosphor

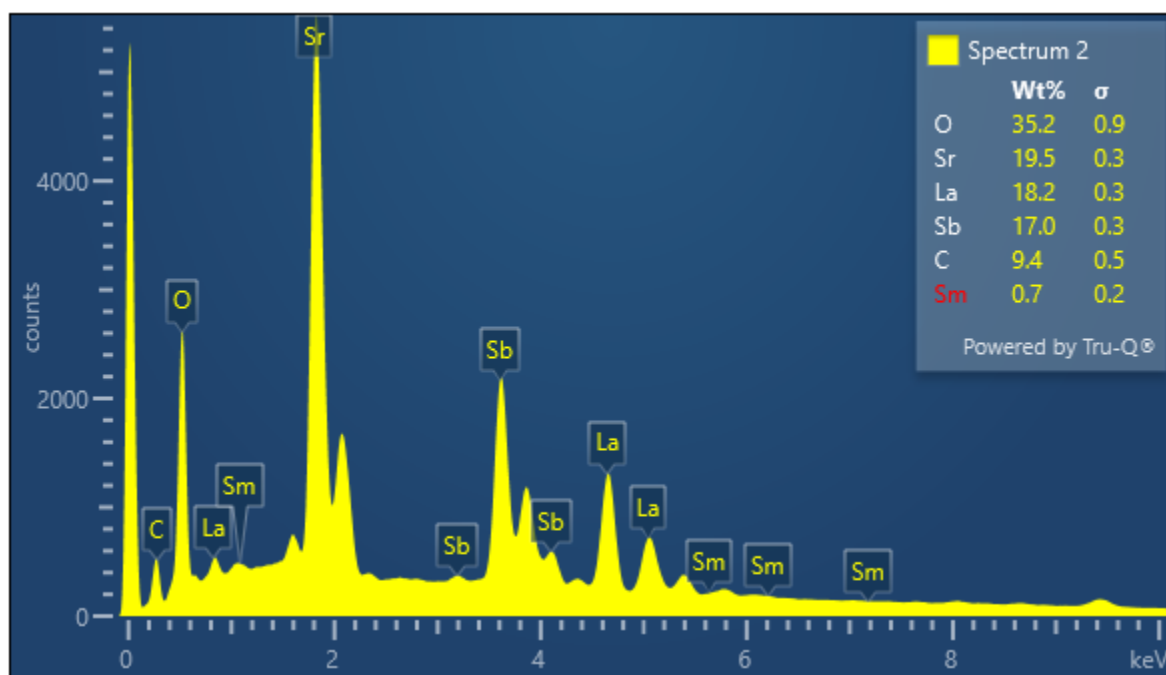


Figure 4.3: EDX image of the doped phosphor

4.3 DIFFUSE REFLECTANCE SPECTRA (DRS):

The optical band-gap is crucial while considering the properties of an LED. We have used the information from the DRS data obtained for $\text{Sr}_2\text{LaSbO}_6:\text{xSm}^{3+}$ (x=1.0, 2.0, 3.0, 4.0, 5.0 mol%) phosphors over the range of 200-600 nm. The DRS spectra as shown in figure-4.4, were converted into a Kubelka-Munk function $F(R)$ form as shown in the equation-3 below[14] to evaluate the optical band-gap value.

$$F(R) = \frac{1-R^2}{2R} = \frac{\alpha}{S} \quad (3)$$

where α denotes the Absorption coefficient, S is the scattering coefficient and R denotes the reflectance of samples. The relation between α and the Energy bandgap E_g is given by the Tauc equation-4 as shown here[4,5,17]:

$$\alpha h\nu = C(h\nu - E_g)^n \quad (4)$$

Here, E_g stands for energy bandgap, $h\nu$ is for the energy photon. C denotes the Energy independent constant (which here is =1), and the value of n can be 1/2 or 2 depending on the type of the transition i.e. direct or indirect respectively. From the above equations, we can see that $F(R)$ has been directly proportional to α ; therefore, the Tauc equation is represented as[4,8]:

$$F(R)h\nu = C(h\nu - E_g)^n \quad (5)$$

The Tauc plot is the graph plotted between $h\nu$ and $[F(R)h\nu]^2$ to evaluate energy bandgap value of $\text{Sr}_2\text{LaSbO}_6:\text{Sm}^{3+}$ phosphor. As we extrapolate the line in the linear region of the plot, we obtain the optical band gap E_g as shown in the figure -4.5. The band gaps of $\text{Sr}_2\text{LaSbO}_6:\text{xSm}^{3+}$ (x=1.0, 3.0, 4.0, 5.0 mol%) were obtained to be 5.46, 5.43, 5.40, 5.38 and 5.36 eV respectively. The decreasing

bandgap can be explained by the development of intermediate energy levels in the rare earth (RE) ions (Sm^{3+}). While increasing the concentration, the expansion caused by the presence of the activator ions in the unit cells of the host lattice results in the narrowing of the valence band and conduction band, which consequently widens the Band gap[4,5,35].

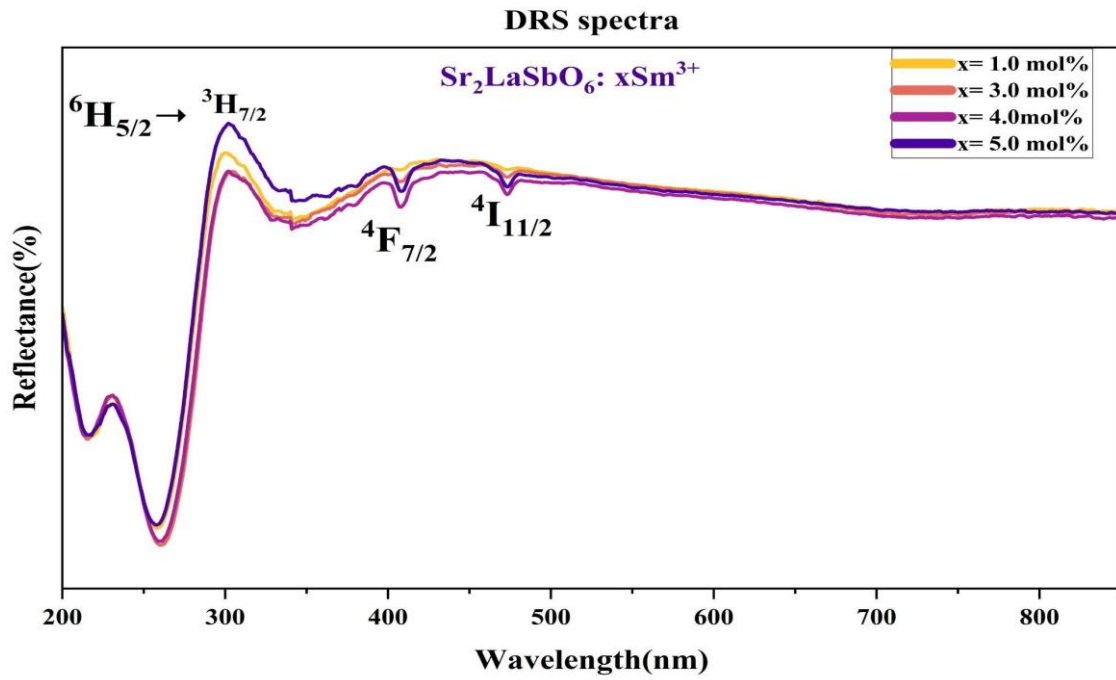


Figure 4.4 : The DRS spectra of $\text{Sr}_2\text{LaSbO}_6$ doped with Sm^{3+} ions at different concentration.

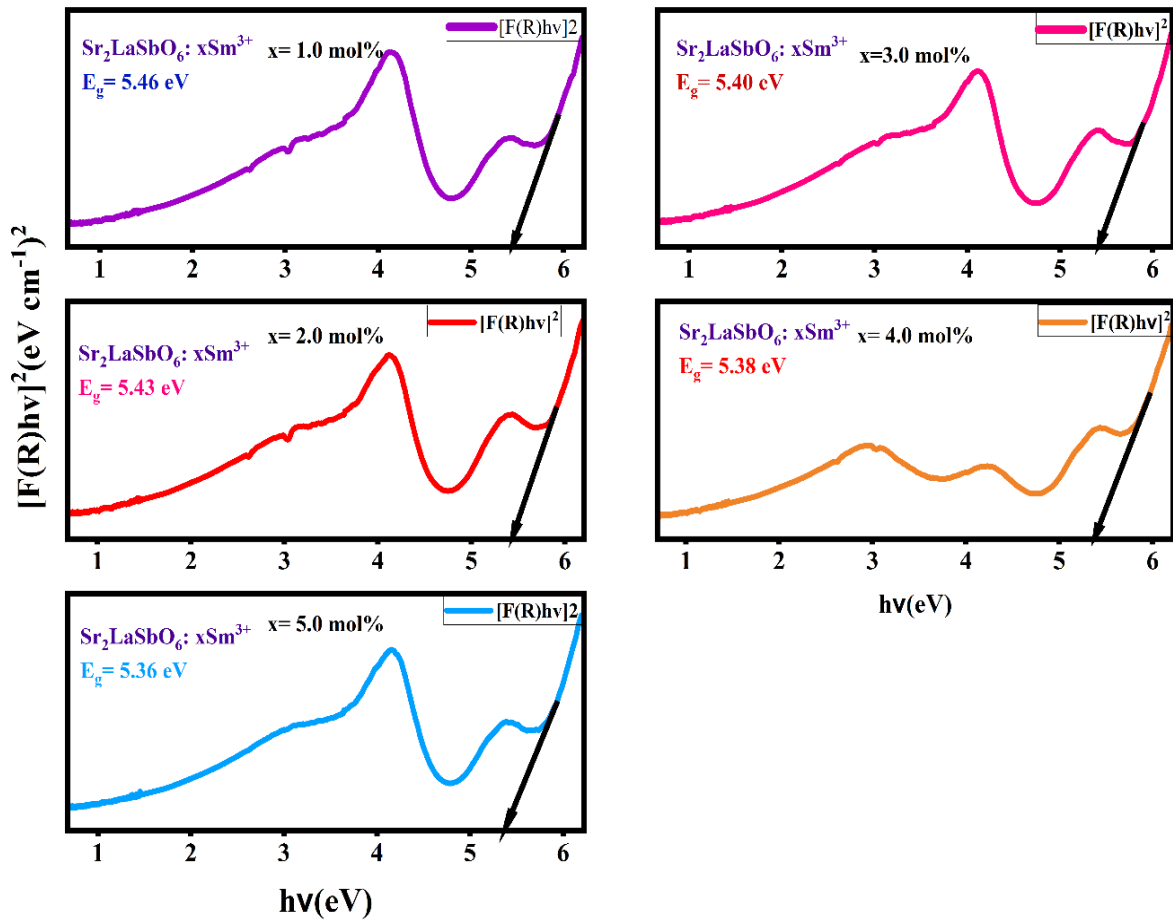


Figure 4.5: The Tauc plots of $\text{Sr}_2\text{LaSbO}_6:\text{xSm}^{3+}$ ($\text{x}=1.0, 3.0, 4.0, 5.0$ mol%) for evaluation of optical band gap

4.4 PHOTOLUMINESCENCE (PL) SPECTROSCOPY ANALYSIS:

In order to investigate the photoluminescent characteristics of phosphors, the excitation spectra of as-prepared Sm^{3+} doped $\text{Sr}_2\text{LaSbO}_6$ phosphor were reported and depicted in Figure-4.6(a). The excitation spectra were recorded in the range of 350-500 nm. The excitation spectrum consists of the $f \rightarrow f$ transitions of Sm^{3+} ions. There is a strong intense peak at 407 nm corresponding to ${}^6\text{H}_{5/2} \rightarrow {}^4\text{F}_{7/2}$. Since the excitation band observed at 407 nm ${}^6\text{H}_{5/2} \rightarrow {}^4\text{F}_{7/2}$ has the highest intensity, the emission study has been prescribed by exciting all the as-prepared Sm^{3+} ions doped phosphor materials at 407 nm [1,4,8,35,36]. The Sm^{3+} ions doped $\text{Sr}_2\text{LaSbO}_6$ phosphors were excited at 407

nm, concurrent emissions at 612 nm were observed. The edged peaks are attributed to the transitions of Sm^{3+} ions from $^4\text{G}_{5/2}$ to $^6\text{H}_{5/2}$, $^6\text{H}_{7/2}$, $^6\text{H}_{9/2}$, $^6\text{H}_{11/2}$, corresponding to the wavelength 569, 612, 654, 715 nm respectively [4,16,27,37]. In the obtained emission spectra, as shown in figure-4.6(b) we observe the sharpest peak at wavelength 612 nm demonstrating the transition from $^4\text{G}_{5/2}$ to $^6\text{H}_{7/2}$, which is considerably more potent. The Sm^{3+} ions hence have 2 potential sites inside the matrix to occupy, provided that the matrix is having double luminescence centres. Which is taken as the possible cause for the splitting of prominent peaks in the emission spectra into two peaks attributed to the stark splitting in the host lattice.[35]

The **Dexter's theory**, which establishes a relationship between photoluminescent intensities and concentration of doping, is applied to determine the type of multipolar interaction with the help of the equation as shown below [4,15,24]

$$\log\left(\frac{I}{x}\right) = A - \frac{s \log(x)}{d} \quad (6)$$

Here, A is a constant while d stands for the dimensions of the compound (which is 3) and I denotes the intensity of emission. The value of s is used to describe the type of interaction as dipole-dipole, dipole-quadrupole, and quadrupole-quadrupole having value closer to 6, 8, and 10 respectively[5,12]. A linearly fitted curve between $\log(1/x)$ and $\log(x)$ has a slope value which is equal to (s/d) as shown in the figure-4.7(b). The calculated value of the s came out to be 5.1 which is fairly close to 6, indicating dipole-dipole interaction as the reason behind the concentration quenching among Sm^{3+} ions in $\text{Sr}_2\text{LaSbO}_6$ phosphors[11,12].

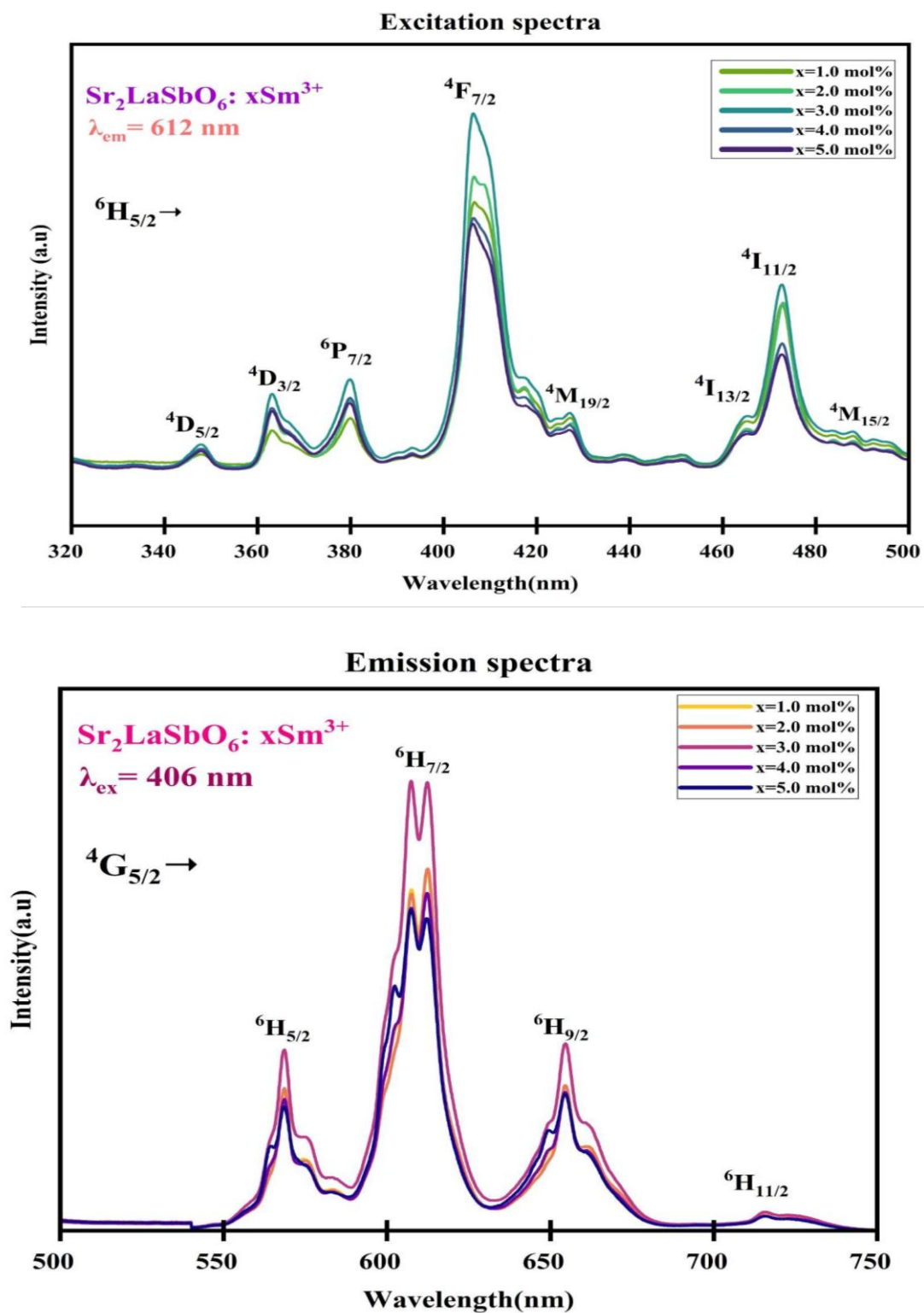


Figure 4.6: (a) The Excitation spectra and (b) The Emission spectra of Sr₂LaSbO₆ phosphor

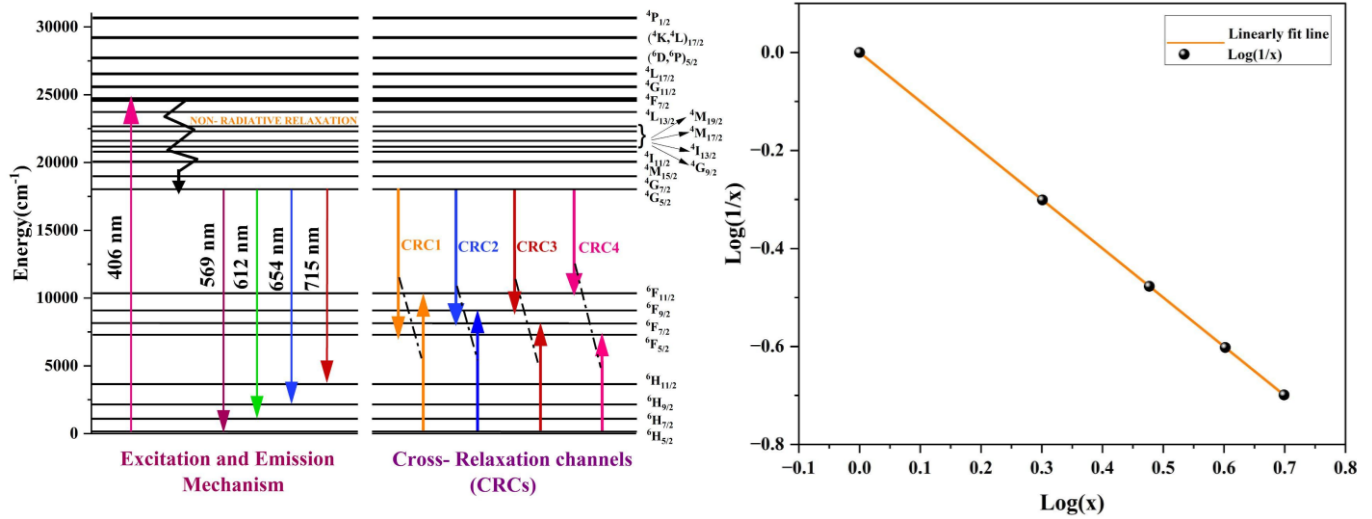


Figure 4.7 : (a) The energy levels and the possible Cross-relaxation channels of $\text{Sr}_2\text{LaSbO}_6:\text{xSm}^{3+}$ phosphor and (b) The plot between $\log(1/x)$ and $\log(x)$

4.5: COLORIMETRY ANALYSIS:

Colorimetry, particularly through the use of CIE coordinates, is a method used to analyze the color output of phosphor materials in a precise and standardized way. When a phosphor is excited typically by UV or visible light—it emits light of a certain color. To understand and quantify this color, researchers measure the emission spectrum of the material and then use it to calculate the CIE (Commission Internationale de l'Éclairage) chromaticity coordinates[24,37].

These coordinates, represented as (x, y) on a two-dimensional chromaticity diagram, help pinpoint the exact color perceived by the human eye. The diagram includes all visible colors, and where the coordinates fall gives a clear visual indication of the material's emitted color. For example, a coordinate near the blue region indicates blue emission, while a point closer to the center might suggest white or near-white light[24,37]. To analyze the colorimetric performance of the $\text{Sr}_2\text{LaSbO}_6:\text{xSm}^{3+}$ ions (x=1.0, 2.0, 3.0, 4.0, 5.0 mol%) phosphor, we determined CIE chromaticity coordinates from the PL data of the phosphor (under excitation 406 nm) as shown in the figure-4.8.

Table -1 displays the calculated CIE coordinates (x,y) and the value of color correlated temperature(CCT) for the series of $\text{Sr}_2\text{LaSbO}_6:\text{xSm}^{3+}$ (x=1.0, 2.0, 3.0, 4.0, 5.0 mol%) phosphors.

The CIE coordinates lie in the **Reddish-orange region** as shown in the figure-4.8, this implies the applicability of the phosphor in solid-state lighting devices and plasma display panels[12,24].

The color purity (CP) of the phosphor is also crucial factor in colorimetry calculations and is utilized for studying the color stability property of the sample. The formula used for calculating color purity is given as follows[8]:

$$\text{Color purity} = \frac{\sqrt{(x - x_{ee})^2 + (y - y_{ee})^2}}{(x_d - x_{ee})^2 + (y_d - y_{ee})^2} \quad (7)$$

Where (x_{ee} , y_{ee}) refers to the equal energy point, while (x,y) are color coordinates of $\text{Sr}_2\text{LaSbO}_6$ phosphor and (x_d , y_d) represent the coordinates of the dominant wavelength. The color purity of the as-synthesised phosphor has been calculated to be 96% under 406nm excitation wavelength. The confirmed high colour purity of $\text{Sr}_2\text{LaSbO}_6$ phosphor highlights its potential for use in a wide range of photonic device applications. The correlated color temperature (CCT) values for the Sm^{3+} -doped samples were found to lie between 1720 and 1725 K. This relatively low CCT range suggests that the phosphor is well-suited as a warm-red light emitter, making it a promising component for white LED applications.[24,37,38]

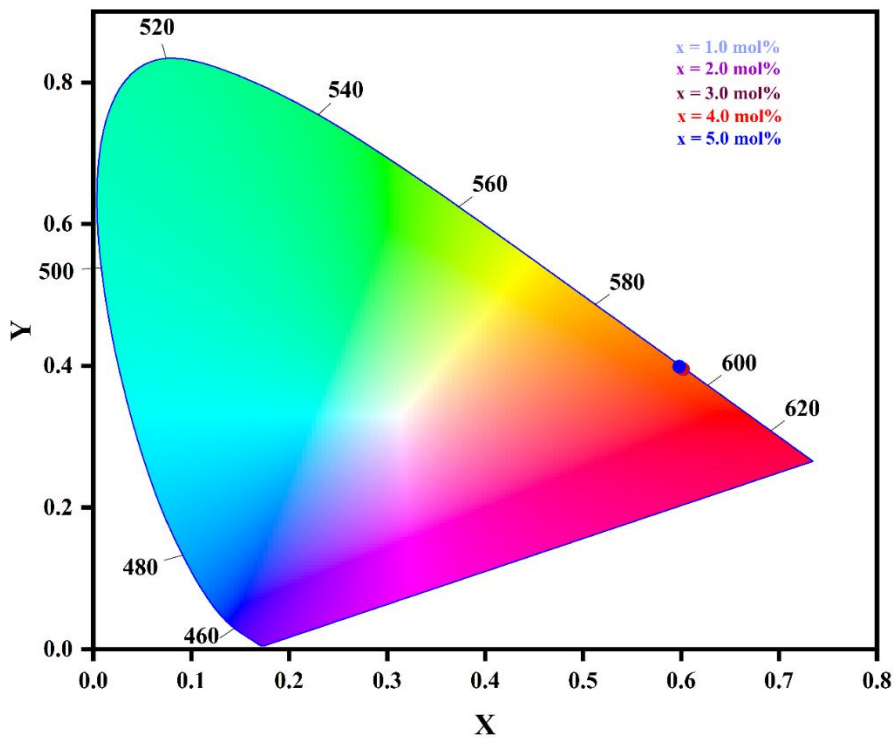


Figure 4.8: CIE chromaticity coordinates of Sm^{3+} ions in $\text{Sr}_2\text{LaSbO}_6$ phosphors.

Table-1: The CIE coordinates and CCT values for Sm^{3+} ions doped $\text{Sr}_2\text{LaSbO}_6$ phosphor

Activator ions conc. (Sm^{3+})	CIE chromaticity coordinates(x, y)	CCT (K)
x= 1.0 mol%	(0.5978,0.3985)	1721.0
x= 2.0 mol%	(0.6007,0.3959)	1725.5
x= 3.0 mol%	(0.5999,0.3969)	1723.7
x= 4.0 mol%	(0.5985,0.3979)	1721.8
x= 5.0 mol%	(0.5963,0.3999)	1720.2

4.6 PL DECAY PROFILE ANALYSIS:

The decay profiles of the synthesised $\text{Sr}_2\text{LaSbO}_6:\text{xSm}^{3+}$ (x=1.0, 2.0, 3.0, 4.0, 5.0 mol%) phosphors are shown in the figure-4.9. The decay data has been recorded for $\lambda_{\text{ex}}=406$ nm and $\lambda_{\text{em}}=612$ nm at the room temperature. The decay plots obtained fitted into various differential exponential equations for each of concentrations. The best fit curve equation was obtained to be the bi-exponential. The luminous intensity is to be depicted by the equation as follows[4,11]:

$$I = I_0 + A_1 \exp\left(\frac{-t}{\tau_1}\right) + A_2 \exp\left(\frac{-t}{\tau_2}\right) \quad (8)$$

where I_0 stands for the initial intensity at $t=0$ and I represents the intensity at time t . A_1 and A_2 stand for the amplitude of the decay constants while τ_1 & τ_2 for the luminescent decay life-times respectively. The following formula helps to estimate the decay lifetime τ_{exp} [4,16]:

$$\tau_{\text{exp}} = \frac{A_1 \tau_1^2 + A_2 \tau_2^2}{A_1 \tau_1 + A_2 \tau_2} \quad (9)$$

The table-2 represents the τ_{exp} values for $\text{Sr}_2\text{LaSbO}_6:\text{xSm}^{3+}$ (SLS:xSm³⁺) phosphor for the concentration x= 1.0, 2.0, 3.0, 4.0 & 5.0 mol. % respectively are represented in the table-2. The decay time is calculated in microseconds range. We observe a decrease in the τ_{exp} values with increase of concentration of Sm^{3+} ions in the synthesised phosphor. This could be demonstrated by the energy transfer among the Sm^{3+} - Sm^{3+} ions at shorter distances between them[24,28]. The equation-10 shown below, we used Auzel's model to investigate the variation of the lifetime with increasing concentration of Sm^{3+} ions[9,16,24].

$$\tau = \frac{\tau_0}{1 + \frac{c}{c_0} e^{-\frac{N}{3}}} \quad (10)$$

here, n represents the number of phonons produced during the relaxation, c stands for the concentration of Sm^{3+} ions, τ_0 is the intrinsic radiative lifetime, while τ stands for the estimated lifetime. We use equation-10 to evaluate the intrinsic lifetime τ_0 . the decay lifetime of Sm^{3+} in SLS

phosphor has been observed to fit well in the Auzel's model as shown in the figure-4.10, the value of intrinsic lifetime τ_0 , is calculated to be 1577.36 μs [16].

Table-2: The excited state lifetime, Non-Radiative rate and luminous efficiency of the SLS:xSm³⁺ phosphor for x= 1.0, 2.0, 3.0, 4.0 & 5.0 mol. %

Sample ID: SLS:xSm³⁺	Excited state-1 lifetime(μs)	Non-Radiative rate (s^{-1})	Luminous efficiency(%)
x= 1.0 mol%	1478.9	42.223	93.75555
x= 2.0 mol%	1335.3	114.941	84.65196
x= 3.0 mol%	1196.2	202.026	75.83365
x= 4.0 mol%	1046.2	321.794	66.33067
x= 5.0 mol%	1019.1	347.303	64.60631

$$\eta = \frac{\tau}{\tau_0} = \frac{A_R}{A_R + A_{nR}} \quad (11)$$

$$\frac{1}{\tau} = \frac{1}{\tau_0} + A_{nR} \quad (12)$$

the luminous efficiency(η) can be calculated by using τ_0 with the help of the equation-11 and 12 as shown above[4,9,16]. Here, A_R and A_{nR} represent the rates of relaxation through radiative and non-radiative transitions respectively. Table-2 shows the luminous efficiency (%) of the as synthesised phosphor, decay lifetime (μ s) and Non-Radiative transition rates as well. The luminous efficiency decreases with the increasing concentration of Sm^{3+} ions[4]. This may be attributed to the phenomenon of concentration quenching in the host lattice due to dominance of Non-Radiative transitions[9,24,28,39].

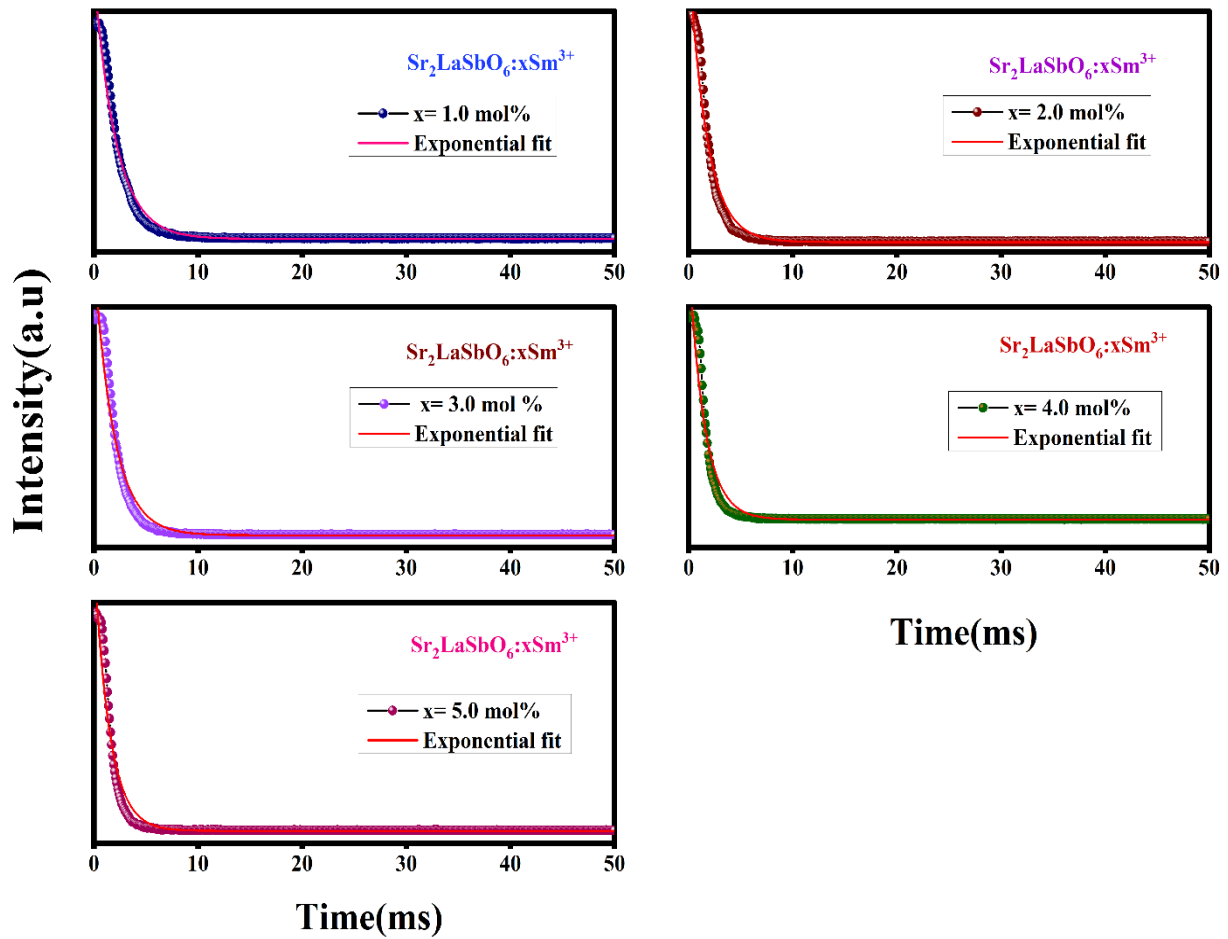


Figure 4.9: The PL decay plots for Sm^{3+} doped $\text{Sr}_2\text{LaSbO}_6$ phosphor at $\lambda_{\text{ex}} = 406$ nm excitation wavelength

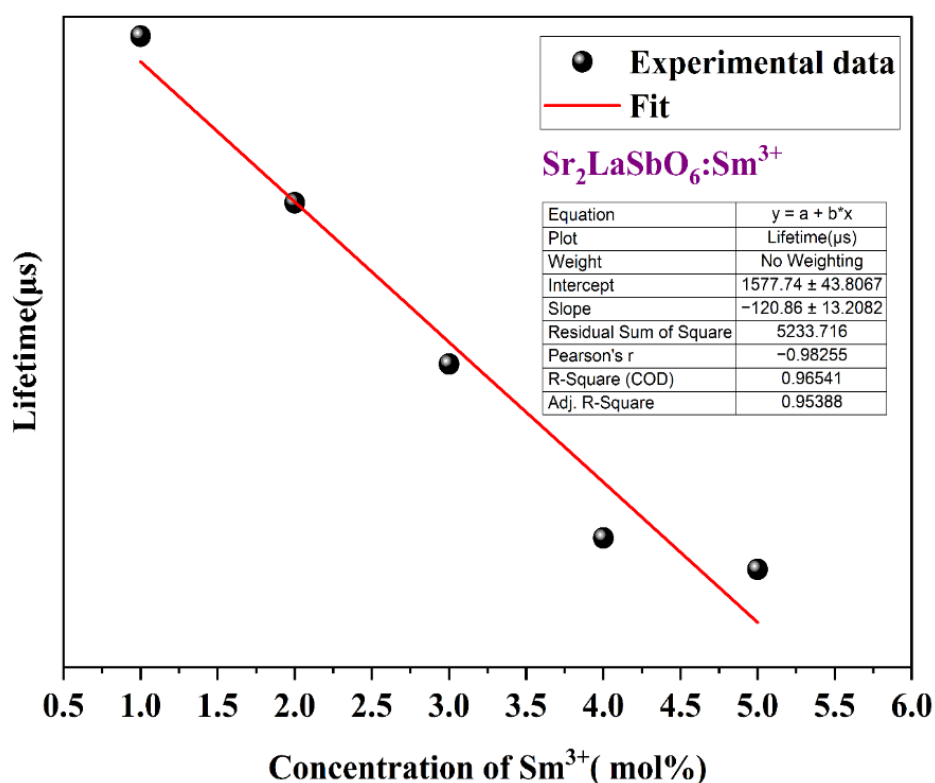


Figure 4.10: The Dependence of lifetime of excited states on the concentration of Sm³⁺ ions according to the Auzel's model

4.7 TD-PL SPECTRAL ANALYSIS:

For analysing the properties like thermal quenching, the TD -PL spectra of Sr₂LaSbO₆: 3.0 mol% Sm³⁺ ion phosphor was monitored at an excitation wavelength of 407 nm for a temperature ranging from 22°C to 175°C. Figure-4.11(a) depicts the TD-PL spectra show that the intensities of the PL peaks decrease with increase in temperature, but also their peak positions stay constant. Figure-4.11(a) illustrates the $^4G_{5/2} \rightarrow ^6H_{7/2}$ transition which is influenced by the temperature, the highest intensity at 22°C is supposed as 100 %. When the temperature is raised to 150°C the intensity is reduced by 20% indicating that the synthesised phosphor maintains 80% of the initial intensity even at high temperature. While after further increasing temperature to 175°C, the emission intensity decreases to 66%, demonstrating that the Sr₂LaSbO₆: x Sm³⁺ (x = 3.0 mol%) phosphor has exhibited relatively high luminous thermal stability[1,25].

Furthermore, the activation energy (ΔE) was determined using the Arrhenius equation[4,16]:

$$I_T = \frac{I_0}{1 + C \exp\left(-\frac{\Delta E}{K_B T}\right)} \quad (13)$$

where I_0 and I_T are the intensities of PL at initial temperature 22°C and temperature T (in Kelvin) respectively, K_B is the Boltzmann constant (8.617×10^{-5} eV/K) and C is an arbitrary constant[4,16]. The value of ΔE has been calculated[1,8,40] with the slope of the linearly fitted plot $\ln [(I_0/I_T)-1]$ vs $1/K_B T$ as depicted in Figure-4.11(b). The ΔE obtained for $\text{Sr}_2\text{LaSbO}_6: x\text{Sm}^{3+}$ ($x=3.0\text{mol}\%$) phosphor is 0.424 eV that is more than previous reported literatures[4,9,16] i.e. $\text{Sr}_9\text{Y}_2\text{W}_4\text{O}_{24}: \text{Sm}^{3+}$ ($\Delta E=0.325$ eV), $\text{Ba}_3\text{ZrNb}_4\text{O}_{15}: \text{Sm}^{3+}$ ($\Delta E=0.191$ eV), $\text{Lu}_{1.93}\text{Ge}_2\text{O}_5: 0.06\text{Bi}^{3+}, 0.01 \text{Sm}^{3+}$ ($\Delta E=0.114$ eV) and $\text{SrBi}_2\text{B}_2\text{O}_7: \text{Sm}^{3+}$ ($\Delta E=0.15$ eV)[4,25,34]. The TD-PL analysis has permitted us to proclaim that the phosphor is relatively thermally stable and revealing its applicability in preparing the visible photonic devices[1,8,40].

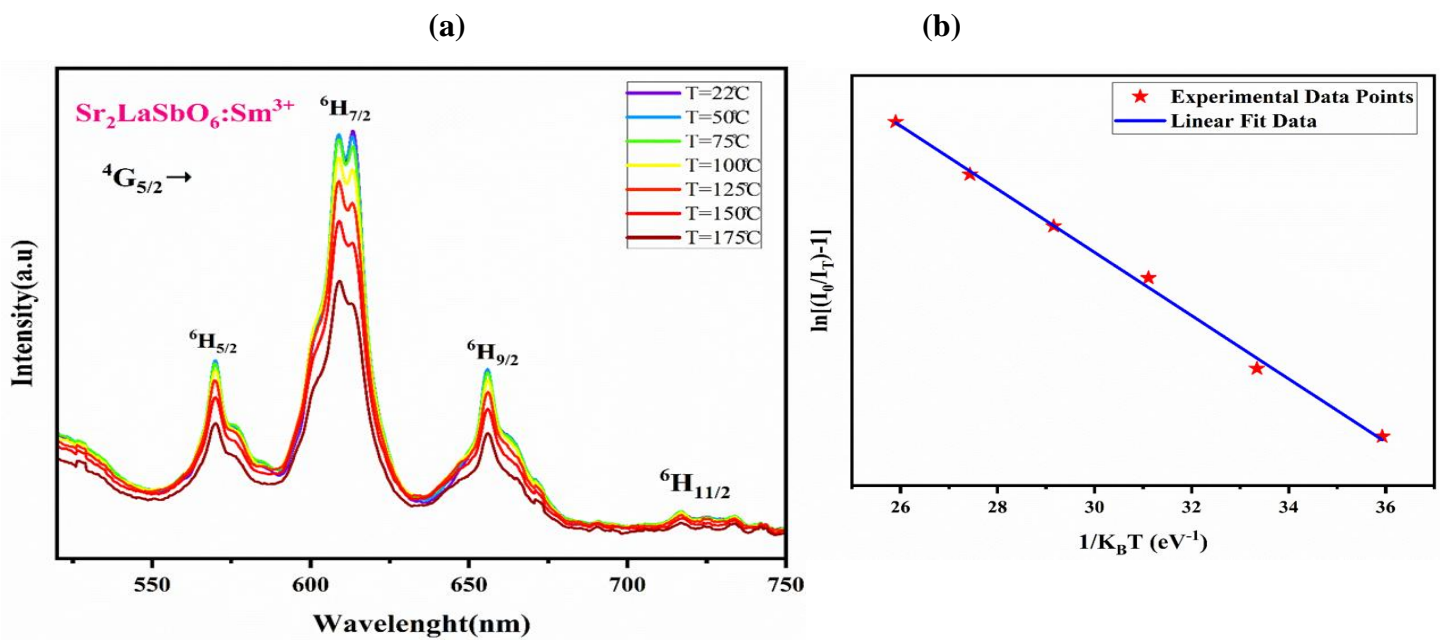


Figure 4.11: (a) The TD-PL intensity variation for 3.0 mol% Sm^{3+} ion doped $\text{Sr}_2\text{LaSbO}_6$ phosphor with temperature range 22°C to 175°C under $\lambda_{\text{ex}}=406$ nm (b) Linearly fitted plot for calculation of Activation Energy

CHAPTER-5:

CONCLUSIONS AND SCOPES OF WORK

In this work, we successfully synthesized a series of Sm^{3+} -doped $\text{Sr}_2\text{LaSbO}_6$ phosphors using a solid-state reaction method and studied their structure, morphology, and photoluminescence properties. The solid state reaction approach has been successfully used to manufacture Sm^{3+} doped $\text{Sr}_2\text{LaSbO}_6$ phosphor. XRD spectra confirms the pure crystalline phase of $\text{Sr}_2\text{LaSbO}_6$. XRD data matches perfectly with the JCPDS. The PL emission were detected for the titled phosphor (under the excitation 407 nm wavelength) $\text{Sr}_2\text{LaSbO}_6$ phosphor emit pure white light. Emission spectra of $\text{Sr}_2\text{LaSbO}_6$ doped with Sm^{3+} at 407 nm excitation wavelength. Most intense emission peak as observed at 412 nm. Optimum concentration for intense emission is 3.0 mol% of Sm^{3+} ions and beyond quenching is achieved. The phase purity of the samples was confirmed by matching them with standard JCPDS data, and the average crystallite size was found to be around 31 nm. The phosphor was shown to have a monoclinic crystal structure with the space group P21/n.

SEM images revealed that the particles were in the micrometer range. Using Tauc plots, we estimated the optical band gap to be between 5.46 and 5.36 eV, suggesting that these materials could be well-suited for photonic applications. Photoluminescence analysis showed four main emission peaks, with the strongest emission at 607 nm, corresponding to the $^4\text{G}_{5/2} \rightarrow ^6\text{H}_{7/2}$ transition when excited with 406 nm light.

We also observed that increasing the Sm^{3+} concentration led to a drop in emission intensity beyond 3.0 mol%, due to concentration quenching caused by dipole–dipole interactions among the Sm^{3+} ions. The CIE coordinates (0.59, 0.39), calculated at 406 nm excitation, fall in the reddish-orange region, and the corresponding CCT values (1720–1725 K) suggest the phosphor is a good candidate for warm-white LED applications.

The decay curves showed a bi-exponential pattern, with lifetime values ranging from 1000 to 1500 microseconds, which decreased with higher Sm^{3+} concentrations due to energy transfer between ions. Additionally, thermal PL analysis demonstrated that the phosphor maintains good stability at elevated temperatures.

Overall, these findings show that Sm^{3+} -doped $\text{Sr}_2\text{LaSbO}_6$ phosphors have promising potential for use in white LEDs and other optoelectronic devices.

SCOPES OF WORK:

Literature survey on the topic area have been carried out. Optimization of synthesis methods. Optimization of activator/sensitizer concentration in the optimized methods. To enhance the emission intensity by varying the excitation wavelength, doping concentration and by co-doping various activators/sensitizers ions. To extend the utility of this phosphor for applications in display devices and other photonic application.

REFERENCES

- [1] P. Dixit, V. Chauhan, S.B. Rai, P.C. Pandey, Realization of neutral white light emission in $\text{CaMoO}_4\text{:4Dy}^{3+}$ phosphor via Sm^{3+} -co-doping, *J. Alloys Compd.* 897 (2022) 162820. <https://doi.org/10.1016/j.jallcom.2021.162820>.
- [2] S1293255820303393, (n.d.).
- [3] S. Pimputkar, J.S. Speck, S.P. DenBaars, S. Nakamura, Prospects for LED lighting, *Nat. Photonics* 3 (2009) 180.
- [4] S. Kumari, A.S. Rao, R.K. Sinha, Structural and photoluminescence properties of Sm^{3+} ions doped strontium yttrium tungstate phosphors for reddish-orange photonic device applications, *Mater. Res. Bull.* 167 (2023). <https://doi.org/10.1016/j.materresbull.2023.112419>.
- [5] S. Kaur, A.S. Rao, M. Jayasimhadri, Spectroscopic and photoluminescence characteristics of Sm^{3+} doped calcium aluminosilicate phosphor for applications in w-LED, *Ceram. Int.* 43 (2017) 7401–7407. <https://doi.org/10.1016/j.ceramint.2017.02.129>.
- [6] A. Fu, A. Guan, D. Yu, S. Xia, F. Gao, X. Zhang, L. Zhou, Y. Li, R. Li, Synthesis, structure, and luminescence properties of a novel double-perovskite $\text{Sr}_2\text{LaNbO}_6\text{:Mn}^{4+}$ phosphor, *Mater. Res. Bull.* 88 (2017) 258–265. <https://doi.org/10.1016/j.materresbull.2016.12.045>.
- [7] V. Sivakumar, U. V Varadaraju, Synthesis, phase transition and photoluminescence studies on Eu^{3+} -substituted double perovskites-A novel orange-red phosphor for solid-state lighting, *J. Solid State Chem.* 181 (2008) 3344.
- [8] L. Shi, S. Wang, Y. jie Han, Z. xin Ji, D. Ma, Z. fei Mu, Z. yong Mao, D. jian Wang, Z. wei Zhang, L. Liu, $\text{Sr}_2\text{LaSbO}_6\text{:Mn}^{4+}$ far-red phosphor for plant cultivation: Synthesis, luminescence properties and emission enhancement by Al^{3+} ions, *J. Lumin.* 221 (2020) 6–14. <https://doi.org/10.1016/j.jlumin.2020.117091>.
- [9] V. Singh, S. Kumari, M. Seshadri, S. Kaur, A.S. Rao, Photoluminescence characteristics of Sm^{3+} activated Y_2SiO_5 orange emitting phosphors, *Solid State Commun.* 378 (2024) 115397. <https://doi.org/https://doi.org/10.1016/j.ssc.2023.115397>.
- [10] H. Dahiya, M. Dalal, A. Singh, A. Siwach, M. Dahiya, S. Nain, V.B. Taxak, S.P. Khatkar, D. Kumar, Spectroscopic characteristics of Eu^{3+} -activated $\text{Ca}_9\text{Y}(\text{PO}_4)_7$ nanophosphors in Judd–Ofelt framework, *Solid State Sci.* 108 (2020) 106341. <https://doi.org/10.1016/j.solidstatesciences.2020.106341>.

- [11] S. Chen, Y. Wang, B. Zhao, B. Deng, Y. Liu, S. Chen, J. Wang, G. Wang, R. Yu, Luminescence properties of novel orange-red-emitting $\text{Gd}_2\text{InSbO}_7\text{:Sm}^{3+}$ phosphor with high color purity for W-LEDs, *J. Lumin.* 237 (2021) 118148. <https://doi.org/10.1016/j.jlumin.2021.118148>.
- [12] M.K. Sahu, M. Jayasimhadri, K. Jha, B. Sivaiah, A.S. Rao, D. Haranath, Synthesis and enhancement of photoluminescent properties in spherical shaped $\text{Sm}^{3+}/\text{Eu}^{3+}$ co-doped NaCaPO_4 phosphor particles for w-LEDs, *J. Lumin.* 202 (2018) 475–483. <https://doi.org/10.1016/j.jlumin.2018.06.002>.
- [13] Z. Zhou, N.F. Wang, N. Zhou, Z.X. He, S.Q. Liu, Y.N. Liu, Z.W. Tian, Z.Y. Mao, H.T. Hintzen, High colour purity single-phased full colour emitting white LED phosphor $\text{Sr}_2\text{V}_2\text{O}_7\text{:Eu}^{3+}$, *J. Phys. D Appl. Phys.* 46 (2013) 35104.
- [14] P. Phogat, V.B. Taxak, R.K. Malik, Crystallographic and Optical Characteristics of Ultraviolet-Stimulated Dy^{3+} -Doped $\text{Ba}_2\text{GdV}_3\text{O}_{11}$ Nanorods, *J. Electron. Mater.* 51 (2022) 4541–4554. <https://doi.org/10.1007/s11664-022-09711-7>.
- [15] Q. Wang, Z. Mu, L. Yang, S. Zhang, D. Zhu, Y. Yang, D. Luo, F. Wu, The synthesis and the luminescence properties of $\text{Sr}_2\text{Ga}_3\text{La}_{1-x}\text{Dy}_x\text{Ge}_3\text{O}_{14}$, *Phys. B Condens. Matter* 530 (2018) 258–263. <https://doi.org/10.1016/j.physb.2017.11.070>.
- [16] P. Rohilla, S. Kumari, Ravita, S. Diwakar, R. Talewar, A. Shandilya, K. Maheshwari, M. Venkateswarlu, A. Prasad, A.S. Rao, Colour tuning in Sm^{3+} activated and $\text{Sm}^{3+}/\text{Eu}^{3+}$ co-activated $\text{SrBi}_4\text{Ti}_4\text{O}_{15}$ phosphors for w-LED applications, *J. Mol. Struct.* 1312 (2024) 138521. <https://doi.org/10.1016/j.molstruc.2024.138521>.
- [17] V. Uma, M. Vijayakumar, K. Marimuthu, G. Muralidharan, Luminescence and energy transfer studies on $\text{Sm}^{3+}/\text{Tb}^{3+}$ codoped telluroborate glasses for WLED applications, *J. Mol. Struct.* 1151 (2018) 266–276. <https://doi.org/10.1016/j.molstruc.2017.09.053>.
- [18] N. Deopa, M.K. Sahu, P.R. Rani, R. Punia, A.S. Rao, Realization of warm white light and energy transfer studies of $\text{Dy}^{3+}/\text{Eu}^{3+}$ co-doped $\text{Li}_2\text{O-PbO-Al}_2\text{O}_3\text{-B}_2\text{O}_3$ glasses for lighting applications, *J. Lumin.* 222 (2020) 117166. <https://doi.org/10.1016/j.jlumin.2020.117166>.
- [19] G. Zhu, Z. Li, F. Zhou, C. Wang, S. Xin, A novel temperature sensitive Sm^{3+} doped niobate orange-red phosphor: The synthesis and characteristic luminescent property investigation, *J. Lumin.* 196 (2018) 32–35. <https://doi.org/10.1016/j.jlumin.2017.12.014>.
- [20] X. Zhang, Z. Zhu, Z. Guo, Z. Sun, L. Zhou, Z. chao Wu, Synthesis, structure and luminescent properties of Eu^{3+} doped $\text{Ca}_3\text{LiMgV}_3\text{O}_{12}$ color-tunable phosphor, *Ceram. Int.* 44 (2018) 16514–16521. <https://doi.org/10.1016/j.ceramint.2018.06.069>.

- [21] S.B. Jiang, H. Yamamoto, M.J.F. Digonnet, J.W. Glesener, J.C. Dries, White LED phosphors: the next step, *Proc. SPIE* 7598 (2010) 759808.
- [22] J. Zhong, M. Xu, D. Chen, G. Xiao, Z. Ji, Novel red-emitting $\text{Sr}_2\text{LaSbO}_6\text{:Eu}^{3+}$ phosphor with enhanced $5D_0 \rightarrow 7F_4$ transition for warm white light-emitting diodes, *Dye. Pigment.* 146 (2017) 272–278. <https://doi.org/10.1016/j.dyepig.2017.07.019>.
- [23] N. Deopa, A.S. Rao, A. Choudhary, S. Saini, A. Navhal, M. Jayasimhadri, D. Haranath, G. Vijaya Prakash, Photoluminescence investigations on Sm^{3+} ions doped borate glasses for tricolor w-LEDs and lasers, *Mater. Res. Bull.* 100 (2018) 206–212. <https://doi.org/10.1016/j.materresbull.2017.12.019>.
- [24] S. Kumari, A.S. Rao, R.K. Sinha, Investigations on photoluminescence and energy transfer studies of Sm^{3+} and Eu^{3+} ions doped $\text{Sr}_9\text{Y}_2\text{W}_4\text{O}_{24}$ red emitting phosphors with high color purity for w-LEDs, *J. Mol. Struct.* 1295 (2024) 136507. <https://doi.org/10.1016/j.molstruc.2023.136507>.
- [25] Q. Li, S. Zhang, W. Lin, W. Li, Y. Li, Z. Mu, F. Wu, A warm white emission of $\text{Bi}^{3+}\text{-Eu}^{3+}$ and $\text{Bi}^{3+}\text{-Sm}^{3+}$ codoping $\text{Lu}_2\text{Ge}_2\text{O}_7$ phosphors by energy transfer of Bi^{3+} -sensitized $\text{Eu}^{3+}/\text{Sm}^{3+}$, *Spectrochim. Acta - Part A Mol. Biomol. Spectrosc.* 228 (2020) 117755. <https://doi.org/10.1016/j.saa.2019.117755>.
- [26] G. Ouertani, M. Ferhi, K. Horchani-Naifer, M. Ferid, Effect of Sm^{3+} concentration and excitation wavelength on spectroscopic properties of $\text{GdPO}_4\text{:Sm}^{3+}$ phosphor, *J. Alloys Compd.* 885 (2021) 161178. <https://doi.org/10.1016/j.jallcom.2021.161178>.
- [27] P. Rohilla, A.S. Rao, Synthesis optimisation and efficiency enhancement in Eu^{3+} doped barium molybdenum titanate phosphors for w-LED applications, *Mater. Res. Bull.* 150 (2022) 111753. <https://doi.org/10.1016/j.materresbull.2022.111753>.
- [28] Deepti, S. Maurya, S. Kumari, P. Rohilla, A. Prasad, A.S. Rao, Dy^{3+} doped $\text{KCa}(\text{PO}_3)_3$ phosphor for white light generation: structural and luminescent studies, *Phys. Scr.* 99 (2024). <https://doi.org/10.1088/1402-4896/ad4def>.
- [29] Sudarta, 済無No Title No Title No Title, 2022.
- [30] V. Sivakumar, U. V Varadaraju, A promising orange-red phosphor under near UV excitation, *Electrochem. Solid-State Lett.* 9 (2006) H35.
- [31] X. Lin, X.S. Qiao, X.P. Fan, Synthesis and luminescence properties of a novel red $\text{SrMoO}_4\text{:Sm}^{3+}, \text{R}^{+}$ phosphor, *Solid State Sci.* 13 (2011) 579.
- [32] J.W. Lee, J.H. Lee, E.J. Woo, H. Ahn, J.S. Kim, C.H. Lee, Synthesis of nanosized $\text{Ce}^{3+}, \text{Eu}^{3+}$ -Codoped YAG phosphor in a continuous supercritical water system, *Ind. Eng.*

Chem. Res. 47 (2008) 5994.

- [33] s10854-021-07301-7 @ doi.org, (n.d.). <https://doi.org/10.1007/s10854-021-07301-7>.
- [34] Y. Niu, F. Wu, Q. zhang, Y. Teng, Y. Huang, Z. Yang, Z. Mu, Luminescence and thermometry sensing of Sr₂InTaO₆: Eu³⁺, Mn⁴⁺ phosphors in a wide temperature range, J. Lumin. 275 (2024) 120748. <https://doi.org/10.1016/j.jlumin.2024.120748>.
- [35] P. Du, X. Huang, J.S. Yu, Facile synthesis of bifunctional Eu³⁺-activated NaBiF₄ red-emitting nanoparticles for simultaneous white light-emitting diodes and field emission displays, Chem. Eng. J. 337 (2018) 91–100. <https://doi.org/10.1016/j.cej.2017.12.063>.
- [36] J. Xie, L. Cheng, H. Tang, X. Yu, Z. Wang, X. Mi, Q. Liu, X. Zhang, Synthesis and photoluminescence properties of NUV-excited NaBi(MoO₄)₂: Sm³⁺ phosphors for white light emitting diodes, Opt. Laser Technol. 147 (2022) 107659. <https://doi.org/10.1016/j.optlastec.2021.107659>.
- [37] S. Xu, D. Zhu, F. Wu, H. Dong, X. Zhang, W. Pang, Z. Mu, High quantum efficiency and excellent thermal stability in Eu³⁺ -activated CaY₂ZrGaAl₃O₁₂ phosphors for wLEDs, Opt. Mater. (Amst). 150 (2024). <https://doi.org/10.1016/j.optmat.2024.115284>.
- [38] R. Yu, Y. Guo, L. Wang, H.M. Noh, B.K. Moon, B.C. Choi, J.H. Jeong, Characterizations and optical properties of orange-red emitting Sm³⁺-doped Y₆WO₁₂ phosphors, J. Lumin. 155 (2014) 317–321. <https://doi.org/10.1016/j.jlumin.2014.06.041>.
- [39] I. Ayoub, V. Kumar, Synthesis, photoluminescence, Judd-Ofelt analysis, and thermal stability studies of Dy³⁺-doped BaLa₂ZnO₅ phosphors for solid-state lighting applications, RSC Adv. 13 (2023) 13423–13437. <https://doi.org/10.1039/d3ra02659k>.
- [40] X.Y. Sun, J.H. Zhang, X. Zhang, S.Z. Lu, X.J. Wang, A white light phosphor suitable for near ultraviolet excitation, J. Lumin. 122–123 (2007) 955.

PLAGIARISM REPORT

shikha and labhansh

Dissertation2 final-report.docx

 Delhi Technological University

Document Details

Submission ID

trn:old::27535:99141552

Submission Date

Jun 3, 2025, 3:06 PM GMT+5:30

Download Date

Jun 3, 2025, 3:46 PM GMT+5:30

File Name

Dissertation2 final-report.docx

File Size

16.7 MB

57 Pages

9,759 Words

57,029 Characters



Page 2 of 63 - Integrity Overview

Submission ID trn:old::27535:99141552

7% Overall Similarity

The combined total of all matches, including overlapping sources, for each database.





Filtered from the Report

- Bibliography
- Quoted Text
- Cited Text
- Small Matches (less than 8 words)

Exclusions

- 1 Excluded Source
- 192 Excluded Matches

Match Groups

-  **60 Not Cited or Quoted 7%**
Matches with neither in-text citation nor quotation marks
-  **0 Missing Quotations 0%**
Matches that are still very similar to source material
-  **0 Missing Citation 0%**
Matches that have quotation marks, but no in-text citation
-  **0 Cited and Quoted 0%**
Matches with in-text citation present, but no quotation marks

Top Sources

- 4%  Internet sources
- 5%  Publications
- 5%  Submitted works (Student Papers)

Integrity Flags

1 Integrity Flag for Review

-  **Replaced Characters**
9 suspect characters on 8 pages
Letters are swapped with similar characters from another alphabet.

Our system's algorithms look deeply at a document for any inconsistencies that would set it apart from a normal submission. If we notice something strange, we flag it for you to review.

A Flag is not necessarily an indicator of a problem. However, we'd recommend you focus your attention there for further review.

Match Groups

- 60 Not Cited or Quoted 7%**
Matches with neither in-text citation nor quotation marks
- 0 Missing Quotations 0%**
Matches that are still very similar to source material
- 0 Missing Citation 0%**
Matches that have quotation marks, but no in-text citation
- 0 Cited and Quoted 0%**
Matches with in-text citation present, but no quotation marks

Top Sources

- 4% Internet sources
- 5% Publications
- 5% Submitted works (Student Papers)

Top Sources

The sources with the highest number of matches within the submission. Overlapping sources will not be displayed.

1	Publication	Deepti, Sandip Maurya, Sheetal Kumari, Pooja Rohilla, Aman Prasad, A S Rao. " Dy...	<1%
2	Submitted works	Texas A&M University, College Station on 2023-10-17	<1%
3	Internet	www.science.gov	<1%
4	Submitted works	Cornell University on 2024-11-27	<1%
5	Publication	Seema, A.S. Rao. "Photoluminescence and energy transfer studies in the Sm3+ an...	<1%
6	Submitted works	University College London on 2017-11-10	<1%
7	Internet	backend.orbit.dtu.dk	<1%
8	Submitted works	IIT Delhi on 2019-05-28	<1%
9	Submitted works	The University of the West of Scotland on 2025-05-05	<1%
10	Publication	"Tailored Light Emitters For Biomedical Applications", Springer Science and Busin...	<1%

11	Publication	Huan Ye, Mingyue He, Tianshual Zhou, Qingfeng Guo, Jialel Zhang, Libing Liao, Le...	<1%
12	Publication	Sheetal Kumari, Pooja Rohilla, Anu ., Srinibas Barik et al. " Linear and nonlinear p...	<1%
13	Publication	Vibha Sharma, Shreya Maurya, A. S. Rao. "Chapter 12 Photoluminescence and Opt...	<1%
14	Submitted works	Universiti Teknologi Malaysia on 2014-10-30	<1%
15	Publication	Weidi Xia, Li Li, Yongbin Hua, Faling Ling, Yongjie Wang, Zhongmin Cao, Sha Jiang...	<1%
16	Internet	www.freepatentsonline.com	<1%
17	Publication	Yuanfeng Zhang, Youzhen Shi, Chaoyong Deng, Min Zhang. " Novel Sm and Eu c...	<1%
18	Publication	Das, Subrata, Che-Yuan Yang, and Chung-Hsin Lu. "Structural and Optical Propert...	<1%
19	Submitted works	University of Houston System on 2019-03-20	<1%
20	Submitted works	National Institute of Technology, Raipur on 2025-05-27	<1%
21	Submitted works	Staffordshire University on 2023-01-07	<1%
22	Submitted works	Universiti Sains Malaysia on 2023-07-26	<1%
23	Internet	netl.doe.gov	<1%
24	Internet	publikationen.bibliothek.kit.edu	<1%

25	Submitted works	OP Jindal University, Raigarh on 2024-03-21	<1%
26	Publication	Rakshit Jain, Rachna Sinha, Mukesh K. Sahu, M. Jayasimhadri. "Synthesis and opti...	<1%
27	Submitted works	Universite de Sfax on 2024-06-01	<1%
28	Internet	worldwidescience.org	<1%
29	Publication	E. Annie Rathnakumari, S. Masilla Moses Kennedy. "Photoluminescence propertie...	<1%
30	Submitted works	The University of Manchester on 2014-05-09	<1%
31	Submitted works	University of New South Wales on 2023-06-10	<1%
32	Internet	www.akink.com	<1%
33	Internet	www.researchgate.net	<1%
34	Submitted works	City University of Hong Kong on 2023-11-03	<1%
35	Publication	K. Naveen Kumar, L. Vijayalakshmi, Gayeon Lee, Gumin Kang, Jiseok Lim, Jungwo...	<1%
36	Publication	Nisha Deopa, Mukesh K. Sahu, Sumandeep Kaur, Aman Prasad, K. Swapna, Vinay ...	<1%
37	Submitted works	Oeiras International School on 2018-12-02	<1%
38	Submitted works	RMIT University on 2024-04-11	<1%

39	Submitted works	Scientific College of Design on 2025-04-13	<1%
40	Submitted works	University of Kent at Canterbury on 2014-04-02	<1%
41	Submitted works	University of Ulster on 2023-07-21	<1%
42	Publication	Yetong Jia, Denghui Xu, Xiangyan Yun, Jun Zhou, Jiayue Sun. "Synthesis and lumin..."	<1%
43	Internet	source.thenbs.com	<1%
44	Publication	Gibin George, G. R. Raghav, Jeetu S. Babu. "Nanotechnology for Mechanical Engin..."	<1%
45	Submitted works	Indian Institute of Technology, Kanpur on 2025-05-01	<1%
46	Submitted works	JNTUA College of Engineering, Anantapur on 2024-05-29	<1%
47	Submitted works	Sefako Makgatho Health Science University on 2024-03-11	<1%
48	Submitted works	Universiteit van Amsterdam on 2019-07-01	<1%
49	Internet	pdfsecret.com	<1%
50	Internet	ufdcimages.uflib.ufl.edu	<1%
51	Internet	www.coursehero.com	<1%
52	Internet	www.dspace.dtu.ac.in:8080	<1%

PROOF OF CONFERENCE PRESENTATION:

6/3/25, 8:46 PM

Gmail - Acceptance Letter for 3rd International Conference on Advanced Functional Materials & Devices for Sustainable Develo...



Shikha Verma <milliochaser@gmail.com>

Acceptance Letter for 3rd International Conference on Advanced Functional Materials & Devices for Sustainable Development (AFMD-2025) at ARSD College

1 message

afmd2025@arsd.du.ac.in <afmd2025@arsd.du.ac.in>
To: milliochaser@gmail.com

16 February 2025 at 02:43

Acceptance Letter – AFMD-2025

Dear Prof./Dr./Mr./Ms. **SHIKHA VERMA**
DELHI TECHNOLOGICAL UNIVERSITY

Greetings from the organizing committee of the International Conference on "Advanced Functional Materials & Devices for Sustainable Development (AFMD-2025)." The conference will be held in hybrid mode* (online & offline) at Atma Ram Sanatan Dharma College, University of Delhi, from March 03-05, 2025. It is being organized by the Department of Physics and Internal Quality Assurance cell (IQAC) of ARSD College.

We are pleased to inform you that the technical committee has accepted your participation, **titled:**

PP-82:-Reddish-Orange Emitting Thermally Stable Sm³⁺ doped Sr₂LaSbO₆ Phosphor for Applications in w-LEDs

Type of Presentation: Poster Presentation:-Online via Google Meet/Zoom

*Program will take place as per following manner:

- *Day-1 Offline Mode at ARSD College*
- *Day 2&3 Online Mode through Zoom of Google Meet*

Kindly confirm your participation by submitting the registration fee in favor of Atma Ram Sanatan Dharma College using the following bank details:

- Bank Name: **ICICI Bank**
- A/c No.: **017101020425**
- IFSC: **ICIC0000171**
- Branch: **Saket, New Delhi**
- SWIFT Code: **ICICINBBNRhi**

PROOF OF POSTER PRESENTATION AND BEST POSTER PRESENTATION:



PROOF OF JOURNAL PUBLICATION:



Shikha Verma <milliochaser@gmail.com>

Rights and Access form Completed form for your article [JPC_116405]

1 message

Elsevier - Author Forms <oaasupport@elsevier.com>
To: milliochaser@gmail.com

10 April 2025 at 13:36

ELSEVIER

Dear Dr Verma,

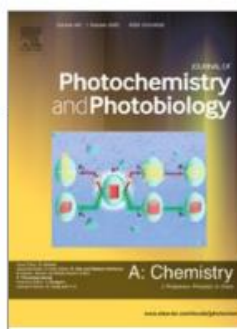
Thank you for publishing your article in Journal of Photochemistry & Photobiology, A: Chemistry. Prof. A.S. completed the Rights and Access Form for your article *Reddish-Orange Emitting Thermally Stable Sm³⁺ doped Sr₂LaSbO₆ Phosphor for Applications in w-LEDs* on April 10, 2025.

The Order Summary is attached to this email. A copy of the Order Summary is also sent to all co-authors for whom we have contact details.

If you have any questions, please do not hesitate to contact us. Quote our article reference JPC_116405 in all correspondence.

Now that your article has been accepted, you will want to maximize the impact of your work. Elsevier facilitates and encourages authors to share their article responsibly. To learn about the many ways in which you can share your article while respecting copyright, visit: www.elsevier.com/sharing-articles.

Kind regards,
Elsevier Researcher Support



Shikha Verma <milliochaser@gmail.com>

Confirm co-authorship of submission to Journal of Photochemistry & Photobiology, A: Chemistry

1 message

Journal of Photochemistry & Photobiology, A: Chemistry <em@editorialmanager.com> 27 January 2025 at 23:25
Reply-To: "Journal of Photochemistry & Photobiology, A: Chemistry" <support@elsevier.com>
To: Shikha Verma <milliochaser@gmail.com>

This is an automated message.

Journal: Journal of Photochemistry & Photobiology, A: Chemistry
Title: Reddish-Orange Emitting Thermally Stable Sm³⁺ doped Sr₂LaSbO₆ Phosphor for Applications in w-LEDs
Corresponding Author: Prof. Allam Srinivas Rao
Co-Authors: Shikha Verma; Labhansh Chaurasia; Sheetal Kumari; Aman Prasad
Manuscript Number: JPHOTOCHEM-D-25-00208

Dear Shikha Verma,

The corresponding author Prof. Allam Srinivas Rao has listed you as a contributing author of the following submission via Elsevier's online submission system for Journal of Photochemistry & Photobiology, A: Chemistry.

Submission Title: Reddish-Orange Emitting Thermally Stable Sm³⁺ doped Sr₂LaSbO₆ Phosphor for Applications in w-LEDs

Elsevier asks all authors to verify their co-authorship by confirming agreement to publish this article if it is accepted for publication.

Please read the following statement and confirm your agreement by clicking on this link: [Yes, I am affiliated.](#)

I irrevocably authorize and grant my full consent to the corresponding author of the manuscript to: (1) enter into an exclusive publishing agreement with Elsevier on my behalf (or, if the article is to be published under a CC BY license, a non-exclusive publishing agreement), in the relevant form set out at www.elsevier.com/copyright; and (2) unless I am a US government employee, to transfer my copyright or grant an exclusive license of rights (or for CC BY articles a non-exclusive license of rights) to Elsevier as part of that publishing agreement, effective on acceptance of the article for publication. If the article is a work made for hire, I am authorized to confirm this on behalf of my employer. I agree that the copyright status selected by the corresponding author for the article if it is accepted for publication shall apply and that this agreement is subject to the governing law of the country in which the journal owner is located.

If you did not co-author this submission, please contact the corresponding author directly at drsallam@gmail.com.

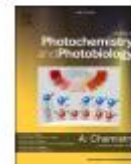
Thank you,
Journal of Photochemistry & Photobiology, A: Chemistry



Contents lists available at ScienceDirect

Journal of Photochemistry & Photobiology, A: Chemistry

journal homepage: www.elsevier.com/locate/jphotochem



Reddish-Orange emitting thermally stable Sm^{3+} doped $\text{Sr}_2\text{LaSbO}_6$ phosphor for applications in w-LEDs

Shikha Verma^a, Labhansh Chaurasia^a, Sheetal Kumari^a, Aman Prasad^b, A.S. Rao^{a,*}

^a Department of Applied Physics, Delhi Technological University, Bawana Road, Delhi 110042, India

^b Department of Physics and Computer Science, Dayalbagh Educational Institute (DEI), Deemed University, Dayalbagh, Agra 282005, India

ARTICLE INFO

Keywords:
XRD
Phosphor
Photoluminescence
CIE coordinates, Decay Kinetics

ABSTRACT

A series of Sm^{3+} ions activated $\text{Sr}_2\text{LaSbO}_6$ phosphors was synthesised using the traditional solid-state reaction (SSR) method. This work presents $\text{Sr}_2\text{LaSbO}_6$ as a novel host material, in contrast to previously examined Sm^{3+} -doped phosphors. It uses its double perovskite structure and LaO_6 octahedral coordination to improve light efficiency and stability, an aspect not fully investigated in perovskite-based phosphors. The phase purity of the synthesized materials was inspected using X-ray diffraction (XRD) characterization technique. The luminescent properties were analysed by photoluminescence emission and excitation (PL) spectra, temperature dependent PL (TD-PL) and decay curves. The XRD results matched the standard JCPDS suggesting that the prepared samples comprise of a pure cubic phase structure. When subjected to 407 nm excitation, the phosphors exhibit intensity peaks at 612 nm corresponding to the transition $^6\text{G}_{5/2} \rightarrow ^5\text{H}_{7/2}$. The PL intensity of the samples increased with the increasing concentration of Sm^{3+} ions until concentration quenching occurred at $x = 3.0$ mol%. The stability and activation energy of the phosphor was calculated with the help of temperature dependant photoluminescence and the phosphor was found out to be highly stable at high temperatures. Most white LEDs use a blue LED chip coated with a yellow phosphor (typically YAG:Ce – Yttrium Aluminium Garnet doped with Cerium). This YAG:Ce phosphor converts some of the blue light into longer wavelengths, producing a broad-spectrum white light. However, this method tends to be weaker in the deep red part of the spectrum, making the light appear cooler and sometimes slightly bluish resulting in high CCT and low CRI. In order to address the prevalent problem of weak red component in white LEDs, which frequently results in low colour rendering index (CRI), this study proposes a Sm^{3+} -doped $\text{Sr}_2\text{LaSbO}_6$ phosphor with high reddish-orange emission. With its efficient 406 nm excitation, the phosphor complements commercial near-UV/blue LEDs and is hence ideal for real-world LED applications. With an activation energy of $\Delta E = 0.424$ eV, it has a strong luminous thermal stability that outperforms several previously reported phosphors, guaranteeing better performance in high-temperature lighting and display technologies. Furthermore, the material has excellent colour purity (96%), putting its emission in the warm red-orange region, which is essential for producing high-quality white light in plasma display panels (PDPs) and solid-state lighting (SSL). These properties make this phosphor a highly efficient red-emitting component, significantly improving the color rendering and performance of w-LEDs.

1. Introduction

In recent years, researchers have been widely interested in white light-emitting diodes (w-LEDs) for use as future light sources due to a variety of features such as high efficacy, use of less energy, machinability, and low environmental pollution [1–4]. Phosphors have extensive number of applications in devices such as plasma display panels, light-emitting diodes (LEDs), fluorescent lamps, medical instruments and high energy detectors. Phosphors have been used to transform

monochromatic light rays into a wide spectrum of light [2,5,6]. This has been made possible by the process known as phosphor conversion. Phosphor conversion is a process in which a LED emits light which is used to excite the phosphor material, which shows emission of light of various wavelengths. Of all these, phosphor-converted white light-emitting diodes (pc-wLEDs) seem to be promising due to their eye-catching luminous performance traits – energy efficiency, large lifespan, durability, good picture quality, brightness, and environmental friendliness [7,8].

* Corresponding author.

E-mail address: drsallam@gmail.com (A.S. Rao).

<https://doi.org/10.1016/j.jphotochem.2025.116405>

Received 27 January 2025; Received in revised form 4 March 2025; Accepted 22 March 2025

Available online 10 April 2025

1010-6030/© 2025 Elsevier B.V. All rights are reserved, including those for text and data mining, AI training, and similar technologies.